PostPrint: Yulei Ma, et al., Journal of Materials Chemistry A, 2021, **9**, 20211-20240
https://doi.org/10.1039/D1TA04693D

Hydrogen sulfide removal from natural gas using membrane technology: A review

Yulei Ma,[a,b,c] Hongfang Guo,[a,b,c] Roman Selyanchyn,[d,e] Bangda Wang,[a,b,c] Liyuan Deng[f], Zhongde Dai*[a,b,c] and Xia Jiang*[a,b,c]

Abstract: Natural gas, having a significantly lower CO_2 emission factor than oil and coal when combusted, is accepted as an important transition fuel towards the carbon net-zero society. To meet the calorific value requirements (≥34.0 MJ/m^3) and reduce possible corrosion to transportation pipelines, acid gases such as CO_2 and H_2S must be removed from raw natural gas. Membrane separation is a promising alternative approach to remove acid gases from natural gases. This paper aims to review the development of various polymer-based membranes and membrane processes for H_2S separation from natural gas. Progress in glassy polymer membranes, rubbery polymer membranes, hybrid membranes and membrane contactors for H_2S removal from natural gas are summarized and analyzed. The H_2S separation performance of various membranes was plotted in one diagram and a new H_2S/CH_4 upper bound was proposed. Challenges of membranes for H_2S separation and prospects of future development are thoroughly discussed.

1 Introduction

Natural gas (NG) is considered to be the cleanest fossil fuel due to the fact that its combustion process produces fewer pollutants [1, 2] and it has lower carbon intensity than other fossil fuels.[3] In 2019, the global NG consumption grew up to 4 trillion cubic meters and accounted for more than 24% of global primary energy use.[4] As shown in **Figure 1**, global NG consumption is currently gradually increasing every year with a rate of ca. 3% per year in a recent decade. The most recent analysis by BP outlined three potential future consumption scenarios considerate of global efforts of battling climate change. In the business-as-usual scenario, steady growth is projected up to 2050, with significant increment in the Americas, China and India, reaching about 6000 billion cubic meters by 2050.[5] In the rapid scenario, consumption growth is projected for another 15 years following the subsequent decline. Interestingly, even in the net-zero scenario, although the demand is expected to peak in the early 2020s, the following decline until 2050 will be only ~35% from the peak value, as the NG is expected to offset the usage of more carbon-intensive fossil fuels - coal and oil. Even in the most climate-conscious scenario, NG is going to be wide across the world, driven primarily by economies in developing countries, mainly in Asia.

Before NG can be sent to the market for sale, purification is normally required as there are always impurities present in raw NG. The composition of raw NG from different reservoirs and geologic layers can be greatly different. However, for all the raw NG, the main component is methane (CH_4). Other components include alkanes (such as ethane and propane), water, carbon dioxide (CO_2) and hydrogen sulfide (H_2S), and some other impurities such as mercaptan (R-SH), nitrogen and helium [6] (as shown in **Table 1**).

Among the components of NG, H_2S and CO_2 are referred to as acid gases. In the presence of water, these two gases will form weak acids,[6] which can cause corrosion of the NG pipeline and increase the transportation cost.[7, 8] Moreover, the removal of acid gases improves the calorific value of NG.[9] Therefore, CO_2 and H_2S must be separated from the NG before entering the transportation pipeline. **Table 2** lists the quality standards of NGs in China, Canada and the USA. As can be seen from **Table 2**, for all the quality standards, the H_2S is always in a low concentration region, China and the USA have more strict standards, the H_2S content in the NG must be lower than 6 mg/m^3, the upper limit for Canada standard is 23 mg/m^3, which is still in the low region.

In addition to corrosion impact on the pipeline, H_2S is highly toxic and harmful to human health. When the concentration reaches 5×10^{-3} mg/m^3, H_2S irritates the eyes, nose and throat; when it reaches 3×10^{-2} mg/m^3, it paralyzes the sense of smell and can be quickly absorbed by the blood; at a concentration of 1 mg/m^3, it can be fatal.[10] **Table 3** lists the H_2S content of several NG wells worldwide. Worth noting that even gas fields only a few hundred kilometers apart can vary greatly in H_2S content. Despite the content of H_2S varies broadly for different reservoirs, most raw NGs need a sulfur removal step to ensure the quality pipeline specifications.

Figure 2 shows a typical flow chart of NG purification. Gas sweetening (removing acid gases) is an important step in NG purification. At present, the dominating method employed in industry to separate H_2S from NG is liquid absorption. Meanwhile, adsorption and membrane separation has been also reported in the literature. In liquid absorption, both physical absorbents and

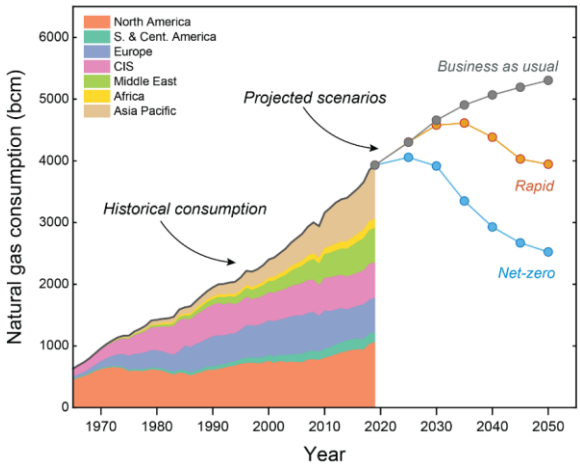

[a] College of Architecture and Environment, Sichuan University, Chengdu 610065, China.
[b] National Engineering Research Centre for Flue Gas Desulfurization, Chengdu 610065, China.
[c] Carbon Neutral Technology Innovation Center of Sichuan, Chengdu 610065, China.
[d] International Institute for Carbon-Neutral Energy Research (WPI-I2CNER), Kyushu University, 744, Motooka, Nishi-ku, Fukuoka 819-0395, Japan.
[e] Research Center for Negative Emission Technology, Kyushu University, 744, Motooka, Nishi-ku, Fukuoka 819- 0395, Japan
[f] Department of Chemical Engineering, Norwegian University of Science and Technology, NO-7491, Norway

Figure 1. Historical global consumption of NG, with three projected consumption scenarios adapted from the BP Energy Outlook.[4, 11]

Table 1. Main Composition of NG.[10, 12-16]

Region	Northeastern Sichuan Basin, China	Western Sichuan Basin, China	Ekofisk, Norway	Süd-Oldenburg, Germany	Tenguiz, Kazakhstan
CH_4 content/ (vol%)	73.71~99.09	81.36~92.9	85	77	42
C_2^+ content/ (vol%)	0.03~0.54	2.44~15.52	12.5	0.1	39
CO_2 content/ (vol%)	0.04~8.93	0~5.67	2	8	2.6
H_2S content/ (vol%)	0.02~17.06	0~8.34	0.001	8	16
N_2 content/ (vol%)		0~2.81	0.4	7	0.8
He content/ (vol%)		0.01~0.071			
Ar content/ (vol%)		0~0.012			
H_2 content/ (vol%)		0~0.09			

chemical absorbents have been applied for H_2S removal. Physical absorption takes advantage of the solubility differences of various gases in the solvent to achieve separation.[10] Common physical absorbents include chilled methanol (Rectisol™ process),[17, 18] N-methyl-2-pyrrolidone (NMP),[18] and polyethylene glycol dimethyl ether (PEGDE, Selexol™ process).[18, 19] Chemical absorption is achieved mainly through the reaction of H_2S with liquid absorbent, and the most widely used chemical absorbent is alkanolamine.[20, 21] In recent years, studies on H_2S absorption using ionic liquids (ILs)[22, 23] and deep eutectic solvents[20, 24] have also been reported.

Similar to liquid absorption, solid adsorbents based on both physical and chemical interactions have been reported for H_2S removal. Physical adsorption separates gas molecules of different sizes through adsorption and retention by the adsorbent, and chemical adsorption relies on the chemical interaction of H_2S with the adsorbent[25]. Materials studied as physical adsorbents include metal oxides,[26] metal-organic frameworks,[27] zeolites,[28] carbon-based adsorbents (e.g., activated carbon,[29] graphene,[30] carbonnanotubes[31]) and composites such as graphene/metal oxides,[32] metal oxides/activated carbon.[33] Adsorption has been applied for H_2S removal at different scales, but it also faces the problem of the high cost of adsorbent regeneration.[10]

Table 2. Minimum calorific value and maximum allowable impurity level for NGs in China, Canada and the USA.

Parameter	China	Canada	USA
Calorific value (MJ/m^3)	34.0	36~41.34	35.40
Total sulfur (mg/m^3)	20	115	114.42
H_2S (mg/m^3)	6	23	6.07
CO_2 (vol%)	3.0	2	2
Hydrogen (vol%)	3.0	Not specified	Not specified
Oxygen (vol%)	0.1	0.4	0.4
Water (mg/m^3)	Not specified	65	112

Compared to liquid absorption and solid adsorption, membrane technology holds intrinsic advantages such as low footprint, linear up-scaling, no moving parts, and no phase change during operation. These factors lead to simplified operation, reduced costs in construction and operation.[13, 34-36] In addition, membrane technology can be used to purify NG with high acid gas content.[37-39] All these advantages make membrane separation a feasible alternative for H_2S removal from NGs. Different membranes and membrane processes have been developed for H_2S separation from NG, including polymeric membranes, mixed matrix membranes and membrane contactors. However, to the best of the authors' knowledge, there is no report summarizing and comparing the separation performances for H_2S over CO_2 and CH_4.

This review paper focuses on the separation of H_2S from NG using membranes and membrane processes. The progress in membrane materials developed for H_2S separation has been summarized and discussed. H_2S separation data under various conditions have been collected and analyzed. Furthermore, an upper bound of H_2S/CH_4 separation have also been proposed, which can be used as a benchmark for future H_2S separation membrane development. In the end, possible future perspectives on membrane material development are proposed. The comprehensive review based on a thorough analysis of literature data in this work provides systematic

technical information for both academic research and industrial applications.

2 Theoretical Background of Membrane Separation

2.1 Separation Mechanisms

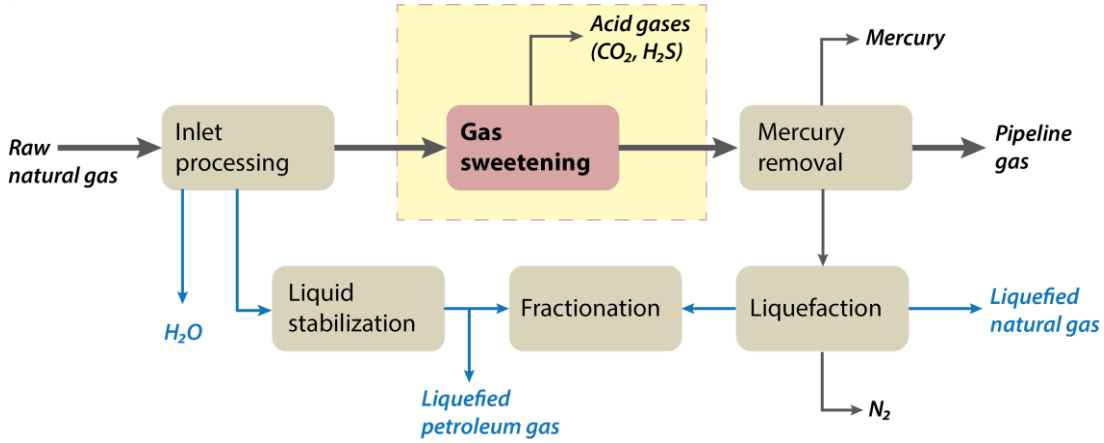

Figure 2. Natural gas purification flow chart, adapted from Ref. [40]. Copyright Elsevier 2012.

Gas separation membranes can be roughly classified into porous membranes and dense membranes.[41] In porous membranes, based on pore size, convective diffusion, the Knudsen diffusion and molecular sieving model can be applied to describe the gas transport; while solution-diffusion and facilitated transport are the two main models applied in dense membranes.[42] The different mass transfer mechanisms are shown in **Figure 3**. All polymeric membranes used for NG sweetening are dense membranes, and the solution-diffusion model dominates. In the solution-diffusion model, the permeability is strongly related to the fractional free volume (*FFV*) of the polymer.[43]

2.2 Solution-diffusion Theory

Solution-diffusion theory is widely used to describe gas transport through a dense polymeric membrane. According to the solution-diffusion model, the gas permeability can be obtained from Fick's law and integrating through the membrane thickness x from 0 to l:[44]

$$P = D \times S \quad (1)$$

where P is the gas permeability [$cm^3(STP)\cdot cm\cdot cm^{-2}\cdot s^{-1}\cdot cmHg^{-1}$], D is the diffusivity coefficient ($cm^2\cdot s^{-1}$) and S is the solubility coefficient [$cm^3(STP)\cdot cm^{-3}(pol)\cdot cmHg^{-1}$] of the gas in the membrane. Gas diffusivity coefficient (D) is a function of the polymeric fractional free volume (*FFV*):[45]

$$D = D_0 \exp\left(-\frac{B}{FFV}\right) \quad (2)$$

where D_0 and B are both empirical constants. The fractional free volume of polymer can be expressed with the following expression:

$$FFV = \frac{V - V_0}{V} \quad (3)$$

where V is the specific volume ($cm^3\cdot g^{-1}$) of the polymer under test conditions and V_0 is the specific volume at absolute zero.

On the other hand, the diffusivity coefficient (D) can be expressed as a function of temperature (T) and activation energy (E_D):[45]

$$D = D_0 \exp\left(-\frac{E_D}{RT}\right) \quad (4)$$

where E_D is the activation energy ($J\cdot mol^{-1}$) of gas diffusion. The diffusivity coefficient generally increases with temperature. The solubility coefficient can generally be expressed as the ratio of the gas concentration [C, $cm^3(STP)\cdot cm^{-3}(polymer)$] in the membrane to the pressure of feed gas (p, Pa), that is,

$$S = C/p \quad (5)$$

The gas solubility coefficient is mainly related to the chemical structure of the polymer and it generally increases as the compressibility of the gas increases. Solubility coefficient is also a function of temperature and it can be described by Van't Hoff equation:[45]

$$S = S_0 \exp\left(-\frac{\Delta H_s}{RT}\right) \quad (6)$$

where S_0 is an empirical constant and ΔH_s is the gas adsorption enthalpy ($J\cdot mol^{-1}$). Since the adsorption enthalpy is generally less than zero, the solubility coefficient decreases with the increase of temperature.

The ideal selectivity ($\alpha_{i/j}$) is the ratio of the permeabilities of the two gases (i and j):

$$\alpha_{i/j} = \frac{P_i}{P_j} = \frac{D_i}{D_j} \times \frac{S_i}{S_j} \quad (7)$$

where D_i/D_j is diffusion selectivity and S_i/S_j is solution selectivity. In practical applications, separation factor ($\beta_{i/j}$) is widely used instead of idea selectivity:

$$\beta_{i/j} = \frac{(y_i/y_j)}{(x_i/x_j)} \quad (8)$$

where x_i and x_j are the mole fractions of component i and j on the feed side, while y_i and y_j refer to component i and j on the permeate side.

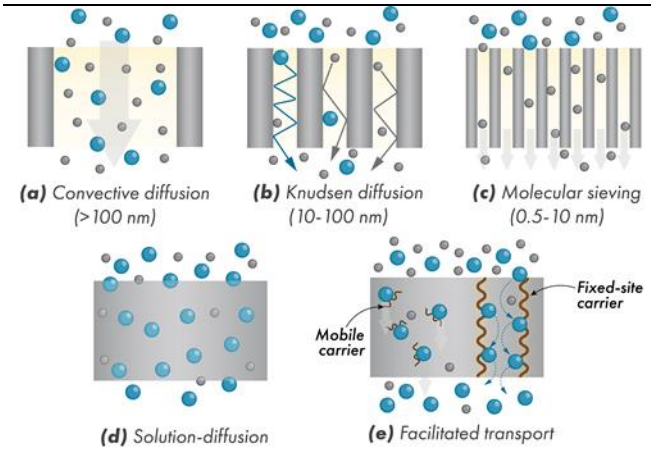

Figure 3. The Transport mechanisms in **(a-c)** porous, and **(d, e)** dense membranes. Characteristic pore sizes of porous membranes are given in brackets.

The separation factor may also be written in terms of the diffusivity and solubility coefficients by including a factor controlled by driving force:

$$\beta_{i/j} = \frac{D_i}{D_j} \times \frac{S_i}{S_j} \times \frac{\Delta p_i/(p_i)}{\Delta p_j/(p_j)} \quad (9)$$

As can be seen from eq.9, the separation factor ($\beta_{i/j}$) approaches the ideal selectivity ($\alpha_{i/j}$) as the partial pressures (p_i and p_j) on the permeate side approach zero.

Gas permeability is generally used to describe the properties of homogenous materials and membranes, and one of the widely used units of permeability is Barrer, where

$$1\ \text{Barrer} = 1\times10^{-10}\ \frac{\text{cm}^3(\text{STP})\cdot\text{cm}}{\text{cm}^2\cdot\text{s}\cdot\text{cmHg}} = 0.33\times10^{-15}\ \frac{\text{mol}\cdot\text{m}}{\text{m}^2\cdot\text{s}\cdot\text{Pa}}.$$

For structurally compels asymmetric or composite membranes, permeance (flux normalized by pressure) is often used to describe gas transport:

$$\text{Permeance} = \frac{P}{l} = \frac{Q}{p_F - p_P} \quad (10)$$

where l is the membrane thickness (cm), Q is the permeate flux ($\text{mol}\cdot\text{m}^{-2}\cdot\text{s}^{-1}$) of the gas, p_F and p_P are the partial pressures (Pa) of the gas on the feed and permeate sides, respectively. And a common unit in practice is the gas permeance unit (GPU):

$$1\ \text{GPU} = 1\times10^{-6}\ \frac{\text{cm}^3(\text{STP})}{\text{cm}^2\cdot\text{s}\cdot\text{cmHg}}$$

2.3 Upper Bound

Permeability (P) and selectivity (α) are the decisive parameters of membrane separation performance, so simultaneously increasing both parameters is the best way to improve the gas separation performance. However, a large number of experiments have shown a "trade-off" between permeability and selectivity, that is, the selectivity decreases with the increase of permeability. In 1991, Robeson[46] collected data of permeability and selectivity for nine gas combinations and found an empirical relation between permeability and selectivity, called upper bound of performance and defines as follows

$$P_i = k\alpha_{i,j}^n \quad (11)$$

where k is referred to as the "front factor" and n is the slope of the log-log plot of the noted relationship. The value of $(-1/n)$ depends on the gas molecular diameters,[47]

$$-1/n = (d_j/d_i)^2 - 1 \quad (12)$$

where d_j and d_i are the kinetic diameters of two gas molecules. And the value of k can be expressed by the formula derived by Freeman,[47]

$$k^{\frac{1}{n}} = \frac{S_i}{S_j} S_i^{-\frac{1}{n}} exp\{\frac{1}{n}\left[b - f\left(\frac{1-a}{RT}\right)\right]\} \quad (13)$$

where S_i and S_j are the solubility constants, a has a universal value of 0.64, b has a value of 11.5 for glassy polymers and 9.2 for rubbery polymers and f is a polymer specific constant.

Since the introduction, the upper bounds have been widely used as a benchmark for comparing gas separation performances. Robeson reported a series of new upper bounds in 2008,[48] and Swaidan and Comesaña-Gándara et al. updated the CO_2/N_2 another one in 2015[49] and 2019.[50] Continuous efforts have been made to push the separation performances to the upper right side of the upper bound.

2.4 Plasticization

Plasticization, a critical issue in polymeric membranes (especially for glassy polymers), refers to the phenomenon of polymer properties change in the presence of plasticizing components (e.g., CO_2 or H_2S). Specifically, the presence of gas in the polymer matrix facilitates rearrangement of polymer segments, increase chain motion and thus *FFV*. As a result, the permeability of all gases increase and selectivity decrease.[51, 52] In the case of NG sweetening, in general, with the increase of H_2S partial pressure in the feed gas mixture, the Langmuir adsorption sites are gradually saturated,[53] leading to the decrease of H_2S permeability. Until reaching a certain critical value of H_2S partial pressure, the permeability of H_2S will increase with the increase of feed gas pressure, and then the plasticization will be considered to have already happened. The pressure corresponding to the inflexion point of the H_2S permeation-feed pressure curve is called the plasticization pressure,[52, 54] shown in a schematic diagram of plasticization (**Figure 4**). When the pressure is less than the plasticization pressure, the H_2S permeation behavior of the membrane can be explained by "dual-mode behavior". A detailed explanation of dual-mode behavior can be found in Ref. [55].

Plasticization results not only in increased permeability of H_2S but also of all other gases present in the feed mixture. Also, a decrease in the selectivity of the membrane is often observed. Many methods, including cross-linking,[36, 38, 56] thermal annealing[57] and blending,[58] have been employed to improve the plasticizing resistance of polymer membranes to enhance their application potential at high H_2S content or high pressure. However, studies have shown that plasticization is not completely detrimental to the gas separation performance of polymer membranes,[59-61] which will be explained in detail in the following sections.

2.5 Physical Aging

Long term stability is another important issue that needs to be considered for gas separation membranes. Most membranes made of glassy polymers will gradually lose their permeance over time,

mainly caused by physical aging, compaction, and oxidation. **Figure 5** shows the variation trend of CO_2 permeability of three glassy polymer membranes with aging time. With the increase of aging time, CO_2 permeability of the membranes decreased continuously, and the CO_2 permeability of poly[1-(trimethylsilyl)-1-propyne]

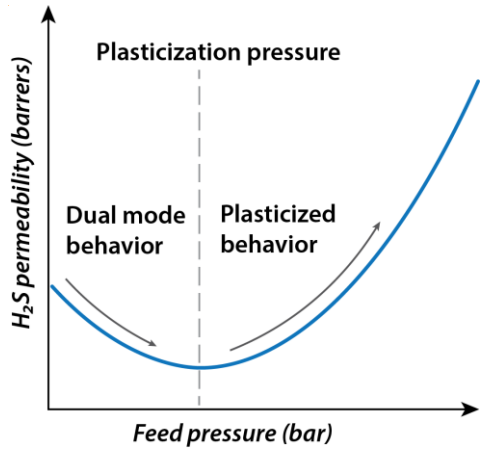

Figure 4. Typical H_2S permeability behavior of glassy polymers, reproduced from Ref. [52, 62]. Copyright Elsevier 2002.

(PTMSP) decreased by 37.4% at 255 days. Generally, thin membranes (≤1 μm) are more likely to suffer age and the gas permeability of thin membranes will decrease at a faster rate than thick membranes (> 10 μm).[63, 64] This may be due to the fact that it's more easily for the *FFV* inside the thin membranes to diffuse to the surface, resulting in a degradation of gas separation performance of thin membranes.[65]

It is generally believed that the polymer membranes will undergo physical aging when it is rapidly quenched from the rubbery state. However, most glassy polymer membranes have unrelaxed free volume, which will drive their transformation towards equilibrium.[66] The main result of this process is the loss of *FFV*, which leads to a decrease in gas permeability. Incorporation of certain fillers in glassy polymers [e.g. functionalized graphene oxide (GO) nanosheets,[67] porous aromatic framework (PAF),[68] α,α'-dichloro-*p*-xylene (*p*-DCX)[69] and three-dimensional covalent organic framework (3D-COF)[70]] or exposing the membrane to a highly soluble penetrant (such as CO_2[66]) can significantly reduce the physical aging of the membranes. In addition, thermal rearrangement[71] and vapor methanol treatment[72] have been proved useful in restoring the gas permeance of aged membranes.

2.6 Competitive Sorption

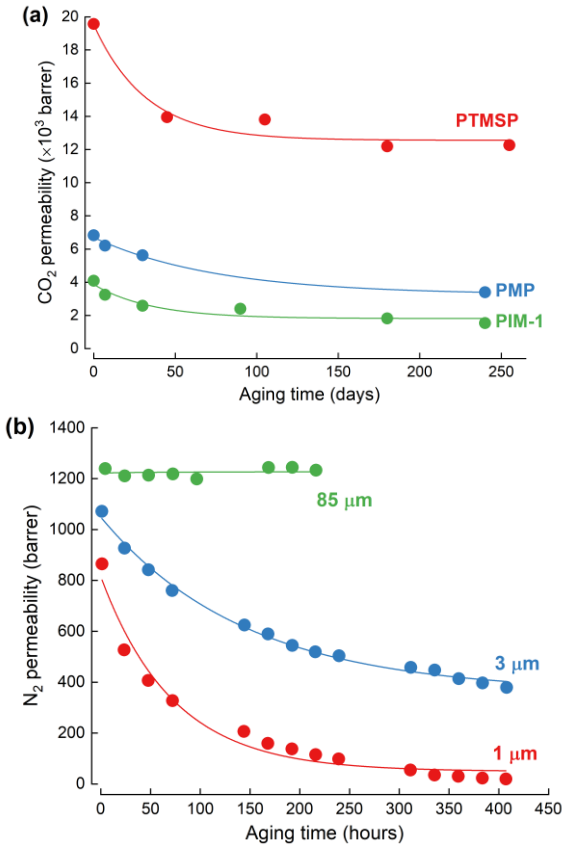

Figure 5. (a) Decrease of CO_2 permeability in PTMSP, PMP and PIM-1 thick membranes due to physical aging, reproduced from Ref. [68], **(b)** Change of the N_2 permeability due to physical aging of PTMSP membranes of different thicknesses (lines in both graphs are added to guide the eyes).[73] Copyright John Wiley and Sons 2014. Copyright American Chemical Society 2001.

In addition to the membrane matrix material, the gas separation performance of the membrane is also affected by the operating temperature, pressure difference and gas mixture compositions. As shown in **Figure 6 (a,b)**, in glassy polymer membranes, the mixed gas solubility and selectivity of the membranes can be quite different from the results obtained by single-component test due to the competitive sorption or some other multi-component effects.[51] Competitive sorption between CO_2 and H_2S in polymers where H_2S can replace the CO_2 adsorbed by the polymer, thus reducing CO_2 permeability and CO_2/H_2S selectivity was reported[74, 75] as given in **Figure 6 (c,d)**. Meanwhile, in many cases, H_2S permeability obtained from mixed gas tests will also be lower than single gas results. However, from an NG sweetening point of view, competitive sorption can sometimes partially offset the negative effects of plasticization.[76-78] In other words, by enhancing the adsorption of polymer membranes to some components in the gas mixture, solubility selectivity can be increased, thus counteracting the decrease of diffusion selectivity caused by plasticization.[77, 78]

3 Polymeric Membranes

3.1 Glassy Polymeric Membranes

Glassy polymers are polymers with a glass transition temperature (T_g) higher than room temperature or operating temperature.[64, 79] Glassy polymer membranes are widely used in NG processing because the polymer rigidity can provide sufficient mechanical strength for membranes, and materials have a large amount of *FFV* for efficient gas permeation.[64]

Cellulose acetate (CA) is a thermoplastic resin obtained by esterification of cellulose with acetic acid as the solvent and acetic anhydride as the acetylating agent under the action of the catalyst. Among various CA membranes, cellulose triacetate (CTA) membranes have a large share in the gas separation membrane market because of their relatively high CO_2/CH_4 selectivity under industrial conditions, commercial readiness, and acceptance by the industry as a low-risk option.[80]

Liu et al.[59] studied the effects of pressure, temperature and toluene concentration in feed gas on NG sweetening performance of CTA hollow fiber membrane (HFM). Firstly, CTA HFM demonstrated higher H_2S permeance (~144 GPU) and H_2S/CO_2 selectivity (~1.3) at high pressure (31.3 bar) due to plasticization. Secondly, they found that operation temperature can be used as a tool to engineer the plasticization benefit and optimize separation performance and economical tuning. A lower temperature is more suitable for NG sweetening. In addition, CTA showed good toluene tolerance. Under lower pressure, due to competitive sorption, the increase of toluene concentration lead to the decrease of H_2S/CH_4 selectivity. At feed pressure of 31.3 bar, the temperature of 35 °C and toluene concentration of 100 ppm, H_2S permeance was 145 GPU, H_2S/CH_4 selectivity was 28, and H_2S/CO_2 selectivity was 1.3. As such, H_2S permeance in CTA HFM was an order of magnitude higher than that of PDMC-CF_3 (~15 GPU) under similar conditions (gas mixture of 25/5/70% $H_2S/CO_2/CH_4$ at 31.0 bar and 35 °C). Also, CTA HFM was more suitable for separating H_2S from CO_2 than PDMC-CF_3 (H_2S/CO_2 selectivity of ~0.6). Achoundong et al.[81] modified CA membranes by grafting method.

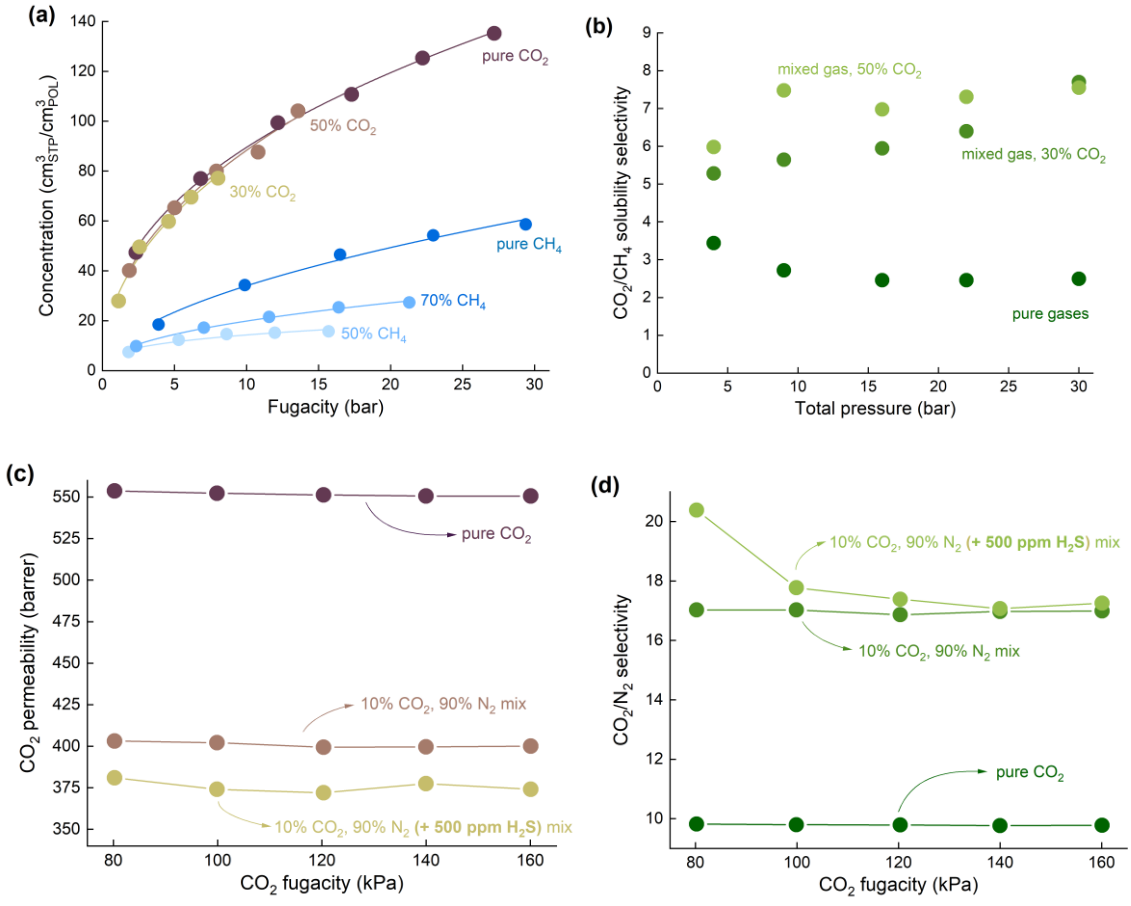

Figure 6. Influence of the gas mixing on **(a)** Sorption isotherms of CO_2 and CH_4 and **(b)** CO_2/CH_4 solubility selectivity in TZ-PIM at 35 °C (adapted from [73, 77]); **(c)** CO_2 permeability and **(d)** CO_2/N_2 selectivity in 6FDA-TMPDA membrane (adapted from [74]). Copyright Elsevier 2019. Copyright John Wiley and Sons 2011.

In the single gas permeation test with a feed pressure of 4.5 bar, H_2S permeability of 170 Barrer was obtained for GCV-modified CA membrane, which is about 40 times higher than that of pure CA (4.5 Barrer). Moreover, the H_2S/CH_4 ideal selectivity of GCV-modified CA membrane (38.0) was also 34% higher than that of pure CA (28.3). GCV-modified CA membranes were also tested using 20/20/60% $H_2S/CO_2/CH_4$ mixture at 6.9~48.3 bar. Within the tested range, the H_2S permeability of the GCV-modified CA membrane remained between 100~110 Barrer, while the H_2S permeability of the pure CA membrane started to increase rapidly from ~3.5 Barrer (at 13.8 bar) to ~37.2 Barrer (at 48.3 bar) due to plasticization. GCV-modification presented improved anti-plasticization performances compared to the CA membrane. In addition, in the range of 6.9~34.5 bar, H_2S/CH_4 selectivity increased with the increase of pressure, but CO_2/CH_4 selectivity decreased in this range, which may be caused by the competitive sorption of H_2S and CO_2.

Polyphenylene oxide (PPO) is an engineering plastic with high strength developed in the 1960s. It has been also reported as gas separation materials shortly after its development.[82] PPO HFMs were used to separate H_2S/CH_4 binary synthetic gas mixtures as well as real NG samples by Niknejad et al.[51]. In the low-sulfur concentration (H_2S <400 ppm) permeation test, the H_2S permeability of the PPO membrane increased with the increase of H_2S concentration in the feed and test pressure, while CH_4 permeability remained almost unchanged. However, the H_2S/CH_4 selectivity increased with the increase of feed pressure and H_2S concentration. An H_2S/CH_4 separation factor of 4.1 was obtained with a feed pressure of 6.89 bar, an H_2S concentration of 401 ppm at 22.5 °C, and the temperature increase had a negligible effect on the separation factor. When H_2S concentration was 968 ppm, the H_2S permeability was significantly reduced, and then increases with H_2S further concentration increment, indicating that plasticization has occurred in PPO with a feed pressure of 3.45 bar. At the same time, it was observed that the CH_4 permeability also increased resulting in a sharp decrease of H_2S/CH_4 separation factor. In the real NG separation test, (H_2S concentration 3360 ppm, temperature 20 °C, feed pressure 6.89 bar), the H_2S/CH_4 separation factor was 3.20, which was lower than the data obtained in synthetic NG tests with similar composition (~5.20), indicating that some components in real natural gas occupied the adsorption sites.

Polyimides (PIs) are the family of polymers fabricated via polycondensation reaction between anhydrides and diamines. They have been widely used for gas separation because of their good chemical stability, excellent mechanical properties and high free volume. However, to make PI membranes more feasible, the separation performance of PI membranes needs to be improved and plasticization needs to be reduced. In the first few decades upon discovery, many new PIs have been developed, while a lot of

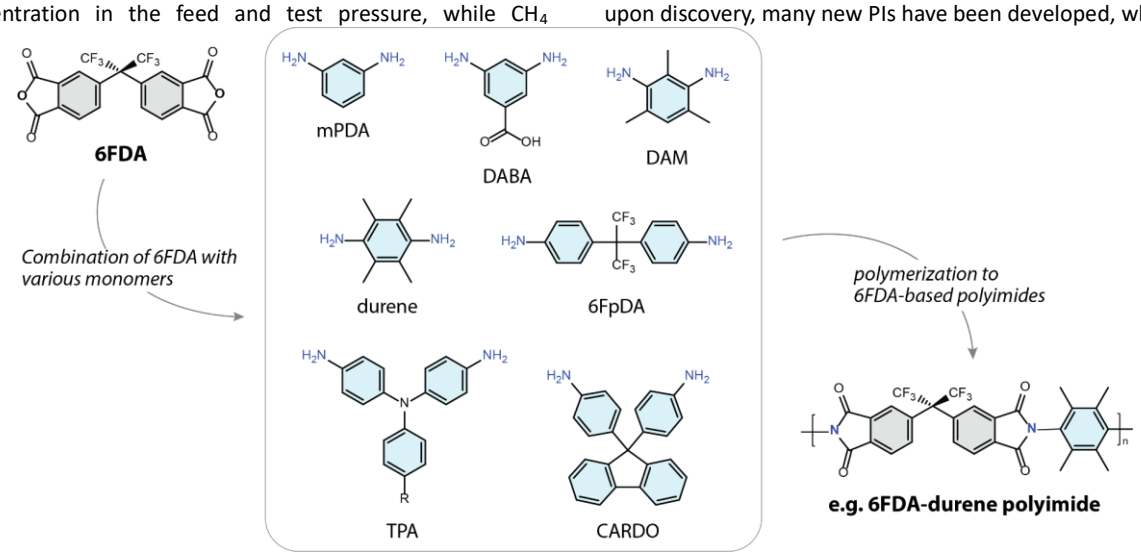

Figure 7. Molecular structures of (a) 6FDA and (b) monomers used to synthesize 6FDA based PIs used for H_2S separation; (c) typical structure of obtained polymers on the example of 6FDA-durene polyimide.[84]

research has focused on physical and chemical modification to improve the gas separation performance of PI membranes.[38, 56, 57, 60, 83] Among those PIs, 4,4'-(hexafluoroisopropylidene)diphthalianhydride (6FDA) based PIs attracted lots of attentions due to easy processibility, relatively good thermal and chemical stability, and good mechanical properties in high-pressure NG.[83, 85] **Figure 7** lists some of the representative 6FDA-based PIs applied in NG sweetening.

Koros and co-workers have conducted a series of studies on the factors affecting the H_2S/CH_4 separation efficiency of 6FDA-based membranes (the molecular formulas of different structural units are shown in **Figure 7**).[36, 38, 39, 56-58, 60, 86, 87] A relatively consistent conclusion was made that the selectivity is mainly controlled by solution differences for H_2S/CH_4, and by diffusion differences for CO_2/CH_4 pair. Therefore, under high pressure, plasticization caused by H_2S and/or CO_2 will reduce CO_2/CH_4 selectivity but improve the H_2S/CH_4 selectivity.[39, 60] First, Kraftschik et al.[57] investigated the annealing temperature on $H_2S/CO_2/CH_4$ separation performance of 6FDA-2,4,6-trimethyl-1,3-diaminobenzene (DAM): 3,5-diaminobenzoic acid (DABA) (3:2) membranes. Permeation test was conducted in as-prepared membranes and membranes annealed at 180 °C and 230 °C. It was found that the plasticizing pressure

increased with the increase of annealing temperature, with an H_2S permeability reduction. At the feed pressure of ~6.6 bar, the H_2S permeability of the unannealed membrane (~58.5 Barrer) was more than two times higher than the membrane annealed at 230 °C (~28.1 Barrer). Under the pressure of 2 bar, H_2S/CH_4 ideal selectivity also decreased with the increase of annealing temperature. A similar trend was observed in H_2S/CH_4 binary mixture (4.98% H_2S in CH_4) permeation tests. An increase of feed pressure from 6.9 bar to 62.4 bar, resulted in an increment in the H_2S/CH_4 separation factor of the membranes annealed at both 180 °C (from 13.3 to 17.7) and 230 °C (from 12.7 to 16.7). In addition, both separation factors were significantly higher than the ideal selectivity (10.4 and 8.3, respectively). When CO_2 was added into the feed gas ($H_2S/CO_2/CH_4$=10/20/70%), although the separation factor of H_2S/CH_4 still increased with the increase of feed pressure, the separation factor of H_2S/CH_4 of the annealed membranes (14.7 for 180 °C annealed and 14.4 for 230 °C annealed) under high pressure is lower than that in binary mixture. In addition, H_2S promotes CO_2/CH_4 separation in 180 °C annealed membrane at low feed pressure. It is believed that it was because H_2S prevented CH_4 molecules from contacting the Langmuir adsorption site, but H_2S did not affect CO_2 molecules. Meanwhile, H_2S induced plasticization was observed under high pressure but it didn't significantly affect H_2S separation efficiency. It is commonly accepted that plasticization would normally lead to the reduction of CO_2/CH_4 and H_2S/CH_4 selectivity, thus reduce the separation efficiency. However, Liu et al.[60] found that plasticization of 6FDA-DAM membrane would only have adverse effects on CO_2/CH_4 separation, but would not restrict H_2S/CH_4 separation. In their study, three different $H_2S/CO_2/CH_4$ mixtures with gas molar ratios of 0.5/20/79.5, 5/45/50 and 20/20/60 were used. When the feed pressure was 6.9 bar, H_2S content significantly affected the H_2S/CH_4 separation performance of 6FDA-DAM and 6FDA-DAM:DABA (3:2) but had little effect on the CO_2/CH_4 separation. Specifically, with the increase of H_2S content from 0.5% to 5%, the H_2S permeability in 6FDA-DAM dropped from 1087 to 332 Barrer, and the selectivity of H_2S/CH_4 decreased from 38.6 to 14.8. The reason for this phenomenon was probably the competitive sorption between H_2S and CO_2 in the membranes. With the increase of H_2S concentration in the feed, the competitive sorption became more intense, leading to a significant decrease in both H_2S permeability and H_2S/CH_4 selectivity. Because glassy polymer membranes with high *FFV* usually undergo physical aging, which affects gas separation performance, Liu et al. further studied the properties of aged 6FDA-DAM membranes. At a low H_2S content (0.5%), the aged (8 months) 6FDA-DAM maintained relatively good H_2S permeability (~640 Barrer) and H_2S/CH_4 selectivity (~40.7) at a pressure of 34.5 bar without plasticization. However, when the H_2S content was 20% and the pressure was ~28.5 bar, it was later observed the aged 6FDA-DAM was also plasticized and lead to a CH_4 permeability increase. After the emergence of plasticization, the selectivity of H_2S/CH_4 remained at ~31.0 and did not decrease even though the pressure was up to 46.0 bar, coupled with an H_2S permeability of ~490 Barrer. Furthermore, with the increase of H_2S permeability, CO_2 permeability decreased sharply, leading to the continuous decrease of CO_2/CH_4 selectivity with the increase of feed pressure, which was also different from the typical trade-off effect. Besides, it was observed that H_2S and CO_2 reduced the CH_4 permeability in 6FDA-DAM and 6FDA-DABA, that is, the mixed gas CH_4 permeability was much lower than that of the single gas test. The causes of these phenomena need to be considered in different ways. The permeation of the $H_2S/CO_2/CH_4$ ternary mixture in 6FDA-DAM has an obvious competitive relationship. When plasticization of 6FDA-DAM occurred, the molecular sieve efficiency decreased, and H_2S/CH_4 and CO_2/CH_4 diffusion selectivity decreased. However, H_2S shows more power in competitive sorption compared to CO_2 and CH_4, which resulted in a higher H_2S solubility. The increased solubility selectivity could offset the reduction in diffusion selectivity and result in improved H_2S/CO_2 selectivity (the H_2S/CO_2 selectivity of the aged 6FDA-DAM was 0.55 at 6.9 bar and 1.64 at 46.0 bar). Therefore, in some cases, the plasticization of 6FDA-DAM may be more favorable for H_2S/CH_4 separation.

Liu et al.[39] synthesized a series of 6FDA-DAM:DABA PIs by regulating DAM and DABA content. As the DAM:DABA ratio increases from 1:2 to 3:2, T_g of the 6FDA-DAM:DABA PIs increases from 357 °C to 375 °C, indicating that DAM doping in the PI backbone strengthens the rigidity of the PI chain. Pure H_2S permeability at a pressure less than 6.9 bar was positively correlated with the DAM doping ratio. Furthermore, although H_2S induced plasticization occurred in all 6FDA-DAM:DABA with the increase of feed pressure, H_2S/CH_4 selectivity was not significantly reduced. In contrast to single H_2S permeation test, in the 50/50 v/v% CO_2/CH_4 mixture, the selectivity of CO_2/CH_4 decreased significantly with the increase of feed pressure, which can be explained by the fact that the selectivity of H_2S/CH_4 is mainly determined by the solubility selectivity.[57] While the rigid PI chain can inhibit the polymer chain packing to a certain extent, which provides more *FFV* and thus increases the adsorption of H_2S, partly offsetting the plasticization induced reduction on the diffusion selectivity of H_2S/CH_4. Liu et al. also investigated the separation of 25/5/70 v/v% $H_2S/CO_2/CH_4$ mixture by DABA membranes at different pressures at 35 °C. With the increase of DAM:DABA doping ratio, the plasticizing pressure of the polymer film was significantly reduced. A typical tradeoff effect was shown for CO_2/CH_4 separation, 6FDA-DAM:DABA (3:2) always had the highest CO_2 permeability and the lowest CO_2/CH_4 selectivity at various test pressure while 6FDA-DAM:DABA (1:2) had the lowest CO_2 permeability and the highest CO_2/CH_4 selectivity. However, DAM:DABA doping had a negligible effect on the separation of H_2S/CH_4. With the increase of the DAM:DABA doping ratio, the permeability of H_2S under high pressure increased, with an unchanged H_2S/CH_4 selectivity. For 6FDA-DAM:DABA (3:2), which has the best H_2S separation performance, H_2S permeability increased from about 35 Barrer to 106 Barrer when feed pressure increased from 6.9 bar to 48.0 bar, with the H_2S/CH_4 selectivity increased from ~17.8 to ~24.5. Furthermore, only at high pressure (48.0 bar), H_2S/CH_4 selectivity (~24.5) of 6FDA-DAM:DABA (3:2) became higher than CO_2/CH_4 selectivity (~22.4). As shown in **Figure 8**, doping more DAM into the 6FDA-DAM:DABA backbone enabled the membrane to have high H_2S permeability while maintaining high H_2S/CH_4 selectivity, which is of great significance for industrial applications.

In order to improve the membrane stability and selectivity, Kraftschik et al.[56] synthesized poly(ethylene glycol) (PEG) monoesterified cross-linkable (PEGMC) membranes based on 6FDA-DAM:DABA (3:2) with three cross-linking agents, diethylene glycol (DEG), triethylene glycol (TEG) and tetraethylene glycol (TetraEG), and then compared the H_2S separation performance of different membranes before and after cross-linking at 280 °C. In the single gas permeation test, the plasticizing pressure of the uncross-linked PEGMC membranes was less than 1 bar, the H_2S permeability was lower than the 6FDA-DAM:DABA (3:2) annealed at 180 °C, and the permeability decreased with the increase of the molecular weight of the cross-linking agents. Cross-linking significantly increased the plasticizing pressure of PEGMC membranes, while it sacrificed H_2S permeability. The decrease of H_2S permeability in the DEG-cross-linked membrane was particularly pronounced. In the single gas test at the same pressure of 7 bar, the H_2S permeability of the DEG-cross-linked membrane was reduced by half (from ~50 Barrer to ~25 Barrer) compared to non cross-linked PEGMC. The H_2S/CH_4 ideal selectivity (at 4.5 bar) of three PEGMC membranes was between 8.3 and 9.0, which is lower than that of unmodified 6FDA-DAM:DABA (3:2) (10.4), and far lower than that of CO_2/CH_4 ideal selectivity under the same conditions (30.1~34.2), indicating that this kind of cross-linked membrane might not be suitable for H_2S related applications. Similar results were obtained in 20/20/60% $H_2S/CO_2/CH_4$ mixed gas permeation tests. The H_2S permeability of the unmodified PI membrane was always higher than that of the three cross-linked PEGMC membranes. A similar trend was observed for H_2S/CH_4 selectivity when feed pressure was lower than 42 bar. When the feed pressure was higher than 48 bar, the H_2S/CH_4 selectivity of the TEG-cross-linked PEGMC membrane was higher than that of the neat PI membrane. When the feed pressure was 62 bar, the H_2S/CH_4 and H_2S/CO_2 selectivity of triethylene glycol monoesterified cross-linkable (TEGMC) membrane and the neat PI membrane was ~23.5, ~0.8 and ~23.0, ~1.2, respectively. Thus, although the cross-linking did improve the anti-plasticization resistance of 6FDA-DAM:DABA (3:2) membranes, it significantly reduced the separation performance of H_2S, possibly due to reduced solubility of H_2S in the cross-linked polymer.

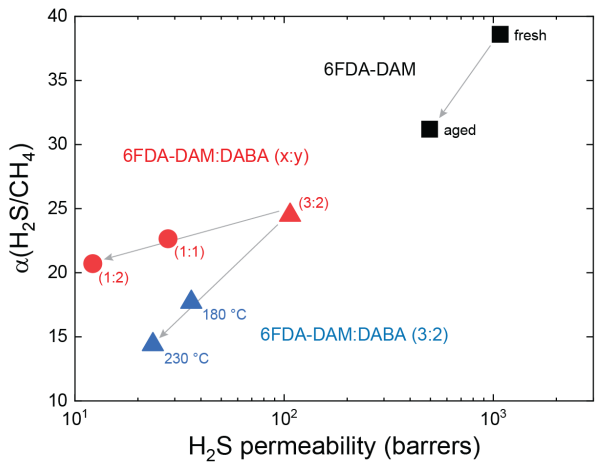

Figure 8. Dependence of H_2S/CH_4 separation performance of 6FDA-DAM:DABA co-PI membranes and derivatives from composition and annealing temperature, adapted from [39, 57, 60].

Based on Kraftschik's et al. research, Badu et al.[36] studied the effects of TEG monoesterified cross-linking and further post-treatment - deposition of a polydimethylsiloxane (PDMS) layer on the surface of fibers, on the H_2S separation performance of 6FDA-DAM:DABA(3:2) HFMs. In the single gas permeation test, the plasticizing pressure of the uncross-linked TEGMC was about 3.1 bar, and it increased to about 4.5 bar in cross-linked and PDMS post-treated TEGMC, but the H_2S permeability of the cross-linked TEGMC was almost two times lower compared to uncross-linked TEGMC. In the 5/45/50% $H_2S/CO_2/CH_4$ ternary gas mixture permeation test, the H_2S permeability was almost the same as in untreated TEGMC and PDMS post-treated TEGMC. However, due to plasticization, CH_4 permeability in untreated TEGMC increases rapidly under higher pressure, resulted in a decrease of H_2S/CH_4 selectivity from 20 (at 6.9 bar) to 12 (at 48.3 bar). In contrast, the H_2S/CH_4 selectivity of PDMS post-treated TEGMC increased from 24 (at 6.9 bar) to 28 (at 20.7 bar) and kept unchanged in higher pressures (from 20.7 bar to 48.3 bar). In a more aggressive 20/20/60% $H_2S/CO_2/CH_4$ ternary gas mixture permeation test, the PDMS treated membrane showed lower H_2S/CH_4 selectivity (20~23) than in a mixture containing 5% H_2S. With the increasing pressure, the H_2S/CH_4 selectivity of the PDMS treated membrane did not decrease significantly, and the membrane showed good stability over time; on the other hand, the H_2S/CH_4 selectivity of untreated membranes decreased to less than 15 at 13.8 bar. Overall, the study demonstrated that PDMS modification is an effective method to improve the anti-plasticization ability of the TEGMC membranes.

Based on previous work,[88, 89] Liu et al.[38] evaluated the H_2S separation performance and stability of rigid cross-linked and uncross-linked propanediol monoesterified cross-linkable 6FDA-DAM:DABA(3:2) with bulky $-CF_3$ side groups (PDMC-CF_3) HFMs under high H_2S concentration. In the single gas permeation test, both membranes experienced plasticization at 3.4 bar. With the pressure increase from 3.4 bar to 6.9 bar, H_2S permeance of uncross-linked PDMC-CF_3 increased from ~13.4 GPU to ~18.4 GPU, larger than that of the cross-linked membrane (from ~13.0 GPU to ~15.2 GPU), proving that cross-linking improved the anti-plasticization performance of PDMC-CF_3. In the ternary mixture containing 0.5% H_2S, the acid gas separation performance of the two PDMC-CF_3 membranes was almost the same, and neither of them was plasticized below 31.0 bar. Under the highest pressure of 31.0 bar, the H_2S permeance was ~27 GPU, the H_2S/CH_4 selectivity was ~30 and the H_2S/CO_2 selectivity was 1. When H_2S content rose to 20~25%, the uncross-linked membranes underwent significant plasticization at 13.8 bar. In addition, cross-linking had little effect on permeance. For H_2S, the H_2S/CH_4 selectivity of the cross-linked membrane was slightly lower than that of the uncross-linked membrane, which is tantamount to sacrificing selectivity to maintain stability. For CO_2, cross-linking had no significant effect on CO_2/CH_4 selectivity, which might be due to competitive sorption between H_2S and CO_2. By comparison, it was found that PDMC-CF_3 had the highest H_2S and CO_2 permeance and H_2S/CH_4 selectivity

when H_2S content was 0.5%, indicating that PDMC-CF_3 may be a good membrane material for the purification of NG with low-sulfur content.

Vaughn et al.[58] studied the effect of H_2S on the CO_2/CH_4 separation performance of 6FDA-3-amino-4-methyl benzoic acid (3ABA)-4,4-hexafluorisopropylidene dianiline (6FpDA) (6F-PAI). Since H_2S has a higher capacity to occupy the Langmuir adsorption site than CO_2, it reduces the solubility of CO_2 in 6F-PAI,[76] and the selectivity of CO_2/CH_4 decreases accordingly. Within the test pressure range (13.8 ~ 68.9 bar), 6F-PAI did not undergo plasticization or swelling and maintained its selectivity, proving the excellent anti-plasticizing ability suitable for actual NG operation conditions.

In another study, Vaughn et al.[86] investigated sour NG transport properties of a series of 6F-PAIs. In the single gas test, low H_2S permeability was obtained in PIs with low fluorine content [e.g., 6FDA-3ABA-DAM (6F-PAI-2) and 6FDA-3ABA-N,N,N',N'-tetramethyl-1,3-propane diamine (TmPDA) (6F-PAI-3)]. In ternary gases test, H_2S permeability and H_2S/CH_4 selectivity in 6F-PAI-1 firstly increase with feed pressure and begin to decrease at about 42 bar, while in 6F-PAI-2, H_2S permeability increases with pressure (from ~2.5 to ~4.1 Barrer) and selectivity significantly decreases (from ~10.1 to ~6.5). Considering that plasticization happened in 6F-PAI-2 at a much lower feed pressure, while the CO_2 and CH_4 permeability of 6F-PAI-2 showed only a slight hysteresis after the removal of H_2S in the feed flow, indicating that there is no large-scale glassy relaxation, but only local destruction of the polymer microstructure. Hysteresis responses in permeability and selective isotherms are also a measure of polymer stability.[58] In addition to the charge transfer complexes (CTCs) formation, the fluorine content in the main chain of the polymer can be used to adjust the H_2S affinity of polymer, higher fluoride content will benefit membrane stability under high H_2S concentration conditions.

Vaughn et al.[87] also studied the influence of H_2S concentration in feed gas on the performance of 6F-PAIs and proved that increasing fluoride content in the main chain of polymers may help to resist the plasticization caused by H_2S.[58, 86] In ternary mixed gas tests, 6F-PAI-2 was plasticized at low H_2S partial pressure (~1.4 bar), and the H_2S/CH_4 selectivity fell below 10 with the increase of feed pressure to 13.8 bar. However, when H_2S partial pressure reaches 11.0 bar, 6F-PAI-1 with higher fluoride content maintains H_2S/CH_4 selectivity higher than 10. After the removal of H_2S from the feed, the 6F-PAI-2 basically returned to the unplasticized state. Therefore, it's believed that 6F-PAI-2 had not suffered structural damage, which is consistent with the previous speculation. Similar to previous studies, the doping of fluorine into the main chain of polymer is an effective method to improve the stability of the underlying membrane in the presence of H_2S.

Yahaya et al.[90] synthesized block co-PIs with 6FDA, 1,3-phenylenediamine (mPDA) and durene. Gas separation performances of the obtained 6FDA-mPDA/6FDA-durene (5000/5000 g/gmol) membranes were investigated using $H_2S/CO_2/N_2/CH_4$ mixed gas with different H_2S content under 34.5 bar. With the increase of H_2S content from 1% to 20%, all four gas permeabilities firstly decreased and then increased. However, even at 20% H_2S content, H_2S permeability was only 10 Barrer, lower than most other 6FDA based membranes. In the quaternary mixed gas test under 34.5 bar, due to competitive sorption,[60] the H_2S/CH_4 selectivity increased from 15 to 23 when H_2S content increased from 1 to 20, while the CO_2/CH_4 selectivity decreased from 37 to 27. In order to further improve the separation performance of the membrane fabricated in ref [90], Yahaya et al.[91] replaced mPDA with rigid 9,9-bis(4-aminophenyl)fluorene (CARDO) polymers, which contain loop or hinge shaped structure in the polymer backbone. In the 10/10/20/60% $H_2S/CO_2/N_2/CH_4$ mixed gas separation test, H_2S permeability of 42.5 Barrer and H_2S/CH_4 selectivity of 20.6 was reported for random co-PI 6FDA-durene:CARDO (3:1) at 34 bar, the permeability was about 8 times that of 6FDA-durene:mPDA[90] under the same condition and the H_2S/CH_4 selectivity was slightly higher (6FDA-durene:mPDA had an H_2S/CH_4 selectivity of ~18.4). With the increase of feed pressure, both H_2S permeability (~41.4 Barrer) and H_2S/CH_4 selectivity (~21) stayed almost unchanged. In the 20/10/10/3/57% $H_2S/CO_2/N_2/C_2H_6/CH_4$ mixed gas test, the H_2S permeability and H_2S/CH_4 selectivity were 47.3 Barrer and 20.9 for 6FDA-durene:CARDO (1:3) membranes. In both test conditions, the H_2S/CO_2 selectivity increased with the feed pressure, however, unlike 6FDA-DAM:DABA,[39, 60] the H_2S permeability and H_2S/CH_4 selectivity of 6FDA-durene:CARDO (1:3) decreased slightly at high pressure.

Considering that the benzene ring of 4,4'-methylenebis(2,6-diethylaniline) (MDEA) can rotate around the central methylene group (-CH_2-) like the benzene ring of CARDO polymer, thus affecting the chain packing, Hayek et al.[92] synthesized 6FDA-durene:MDEA random co-PI polymer. Under 27.6 bar in 20/10/10/1/59% $H_2S/CO_2/N_2/C_2H_6/CH_4$ permeation test, 6FDA-durene:MDEA (1:3) manifested a high H_2S permeability of 112 Barrer, and the H_2S/CH_4 and H_2S/CO_2 selectivity of 21.0 and 1.5, respectively. In contrast, the H_2S/CH_4 selectivity of 6FDA-durene:MDEA (1:3) was close to that of 6FDA-durene:CARDO (1:3), but the H_2S permeability was 2.4 times that of 6FDA-durene:CARDO (1:3). These results showed that the incorporation of MDEA into 6FDA backbone could deliver a promising membrane material that can effectively separate $H_2S/CO_2/CH_4$ at high pressure of 27.6 bar.

After realizing the significant benefit of CARDO polymer for H_2S separation,[90, 91] Alghannam et al.[93] further synthesized 6FDA-CARDO/6FDA-durene, another block co-PI, and studied specifically how did CARDO polymers affect the properties of the membrane. Ten $H_2S/CO_2/N_2/C_2H_6/CH_4$ mixed gas permeation tests with different H_2S content under different pressure were conducted. In all tests, H_2S permeability increased with feed pressure. H_2S/CH_4 selectivity increased first and then decreased in permeation tests with 10% H_2S containing mixtures, while H_2S/CH_4 selectivity decreased with pressure in permeation tests with 20% and 36% H_2S mixture. However, under the same feed pressure, H_2S/CH_4 selectivity increased with the increase of H_2S content. In addition, H_2S/CO_2 selectivity increased with the increase of pressure and H_2S content. When H_2S content was 36%, H_2S permeability of 275.8 Barrer, H_2S/CH_4 selectivity of 20.1 and H_2S/CO_2 selectivity of 1.9 was documented at 27.6 bar. In summary, CARDO polymer not only increased the H_2S permeability but also enhanced the stability of 6FDA-CARDO/6FDA-durene under harsh test conditions. Thus,

6FDA-CARDO/6FDA-durene is a membrane material with great potential for NG sweetening.

In addition to introducing CARDO structure into 6FDA polymer, Hayek et al.[94] also attempted to copolymerize 6FDA-6FpDA, which has high CO_2/CH_4 ideal selectivity (~45 at 30 °C and 1 bar), with 6FDA-durene to prepare a membrane with both high permeability and high selectivity. Unfortunately, 6FDA-6FpDA/6FDA-durene copolymer showed lower performances compared to 6FDA-CARDO/6FDA-durene in separating H_2S. At 34.5 bar, both H_2S permeability and H_2S/CH_4 selectivity of 6FDA-6FpDA/6FDA-durene (P_{H_2S}=26.4 Barrer, α_{H_2S/CH_4}=13.1) were lower than that of 6FDA-CARDO/6FDA-durene.

In addition to the self-standing membranes with high thickness,[91, 93] Yahaya et al.[95] prepared multilayer thin film composite (TFC) membranes with 6FDA-CARDO/6FDA-durene (5000:5000) as the selective layer. PTMSP and polyacrylonitrile (PAN) were employed as gutter layer and support, respectively. In the single gas test, H_2S permeance of the TFC membrane remained almost unchanged (~220 GPU) with feed pressure increase from 24.1 bar to 48.3 bar. In mixed gas tests with 10% H_2S in the feed, the H_2S/CH_4 selectivity of the TFC membrane was slightly lower than that of the pure 6FDA-CARDO/6FDA-durene (5000:5000) membrane under similar pressure, but the H_2S/CO_2 selectivity of the TFC membrane under high pressure (1.9 and 1.8 at 24.1 bar and 48.3 bar, respectively) was much higher than that of the thick membranes (highest H_2S/CO_2 selectivity of 1.3[93]), which may be due to the presence of PTMSP in the TFC. The high H_2S permeance and high H_2S/CO_2 selectivity of this TFC membrane are beneficial for NG purification focusing on H_2S removal.

To further improve gas separation performance of PI membranes, Hayek et al.[96] added *tert*-butyl groups to CARDO diamine, synthesized 9,9-bis(4-aminophenyl)-2,7-di-*tert*-butylfluorene [CARDO(*t*-Bu)] was used to prepare 6FDA-CARDO(*t*-Bu) membrane. H_2S permeability of 6FDA-CARDO(*t*-Bu) was 3.8 times higher than for 6FDA-CARDO under the same pressure in the 22/10/10/3/55% $H_2S/CO_2/N_2/C_2H_6/CH_4$ mixed gas permeation test, due to the presence of the *tert*-butyl groups increasing the *FFV* of the polymer. With the feed pressure increasing from 20.7 bar to 34.5 bar, H_2S permeability of 6FDA-CARDO(*t*-Bu) increased from 101 Barrer to 148 Barrer, while H_2S/CH_4 selectivity decreased from 18.9 to 16.1, and these changes were typical results of plasticization. Despite this, the H_2S/CH_4 selectivity of 6FDA-CARDO(*t*-Bu) was still 10% higher than that of 6FDA-CARDO at 34.5 bar, showing that increasing the *FFV* in PI membranes by introducing functional groups into the polymer chain is a practical and effective approach.

In following work, Hayek et al.[97] synthesized a series of PIs, namely 6FDA-TPA, 6FDA-TPA(NMe_2) and 6FDA-TPA(*t*-Bu), with 6FDA, 4,4'-diaminotriphenylamine (TPA), 4,4'-diamino-4"-(dimethylamino)triphenylamine [TPA(NMe_2)] and 4,4'-diamino-4"-(*tert*-butyl)triphenylamine [TPA(*t*-Bu)] monomers. After that, they explored the effects of two large side groups in the backbone on the gas separation performance of the membrane. At 20.7 bar, the H_2S permeability of 6FDA-TPA(*t*-Bu) was a bit higher than 6FDA-TPA (54.82 Barrer) and reached 68.14 Barrer, while the H_2S/CH_4 selectivity was 18.3, which was almost the same as 6FDA-TPA (18.0). When feed pressure increased to 34.5 bar, both H_2S permeability and H_2S/CH_4 selectivity of 6FDA-TPA(*t*-Bu) were slightly lower than to 6FDA-TPA (67.08 Barrer and 17.8, respectively). Through the change in CH_4 permeability, it is found out there is significant plasticization in both membranes, which offsets the advantage of H_2S/CH_4 separation brought by the larger side chain of 6FDA-TPA(*t*-Bu).

Recently, Hayek et al.[98] prepared the membranes with polyoxadiazole (POz-CF_3) for NG sweetening due to the high CO_2 permeability and CO_2/CH_4 ideal selectivity of POz-CF_3.[93] However, in the mixed gas test with 20% H_2S in the feed, POz-CF_3 showed a disappointing H_2S/CH_4 separation performance: H_2S permeability of 38.8 Barrer and H_2S/CH_4 selectivity of only 5.2 was documented under 48.3 bar. It was believed that the sharp decrease in separation performances is due to severe competitive sorption. Combined with the previous research experience,[93] Hayek et al. functionalized POz-CF_3 with 4-aminophenol and a new polytriazole was obtained and named as FPT-Ph(OH). At 48.3 bar, the H_2S permeability (~119 Barrer) and H_2S/CH_4 selectivity (~21.3) of FPT-Ph(OH) was 3.1 and 4.1 times higher than POz-CF_3, respectively. H_2S/CO_2 selectivity also increased from less than 1.0 to 1.5. Unlike normal 6FDA-based PIs, the H_2S permeability and H_2S/CH_4 selectivity of FPT-Ph(OH) decreased with increasing feed pressure, while the H_2S/CO_2 selectivity remained basically unchanged. This may be because the intense competitive sorption simultaneously reduced the permeability of H_2S and CO_2, and the decrease ratio of H_2S and CO_2 permeability was almost the same, resulting in almost no change in H_2S/CO_2 selectivity.

Microporous polymers are ideal membrane materials for gas separation because their tunable cavity size can sieve gas molecules, and their large internal surface area is conducive to the adsorption and diffusion of gas molecules.[99] Polymers of intrinsic microporosity (PIMs) is a class of polymers with high rigidity and twisted molecular structure.[100, 101] Because of their high free volume and good processability, PIMs are especially suitable for manufacturing separation membranes,[83, 102] and their molecular structure enables them to have microporous structures in the range of 6 ~ 10 Å, with high gas permeability and moderate selectivity for O_2/N_2 and CO_2/CH_4.[103, 104] However, when it comes to H_2S/CH_4 separation, even though the rigidity of the polymer chain has been greatly improved, as there is no interaction between the polymer chains, most PIMs membranes show reduced H_2S/CH_4 selectivity in high-pressure gas mixtures.[105]

The effect of the side branch on the gas separation performance of triptycene based PIM membrane was studied by Ghasemnejad-Afshar et al.[106] using various simulation methods. In their research, four side branches, $-CH_3$, $-CF_3$, $-C_3H_7$ and $-C_4H_9$, were taken into consideration. As the number of carbon atoms in the side branch increased from one to four, the stiffness of the polymer chain increased and deformed the polymer chain packing, so that the *FFV* increased. The PIM with $-C_4H_9$ as the side branch would have the maximum microcavity volume. In the single gas permeability simulation, the H_2S permeability increased with the length of side branches, thus PIM with $-C_4H_9$ has the highest permeability. In binary mixture gas simulation, PIM with $-C_4H_9$ also shows the

highest H_2S/CH_4 selectivity, but the H_2S/CH_4 selectivity of PIM with $-CF_3$ exceeds that of PIM with $-C_3H_7$, which is due to the fact that there is a strong interaction between $-CF_3$ moiety and H_2S. Even though there is a certain deviation between the simulated permeability and selectivity and the experimental results, these simulation results provide useful guidance for the synthesis and modification of PIMs.

Yi et al.[83] prepared and tested membrane from novel thermally annealed hydroxyl-functionalized PI with intrinsic microporosity (PIM-6FDA-OH) (chemical structure shown in **Figure 9**, synthesized by Ma et al.[107]). In the single gas permeation test, H_2S-induced plasticization was observed under the feed pressure of 4.5 bar, and the permeability of H_2S was 33.7 Barrer, which was higher than the data obtained from cross-linked PEGMC under similar feed pressure (21.8 Barrer),[56] and the H_2S/CH_4 ideal selectivity was 7.1, slightly lower than the cross-linked PEGMC (9.0).[56] In the mixed gas permeation test with 15/15/70% $H_2S/CO_2/CH_4$ mixture as feed, PIM-6FDA-OH readily manifested H_2S-induced plasticization below the minimum test pressure (7 bar). The H_2S permeability increased rapidly from 24.2 Barrer to 63.5 Barrer with the feed pressure increase from 6.9 to 48.3 bar. It is worth noting that the CO_2 permeability decreased rapidly from 89.1 Barrer to 59.0 Barrer when the feed pressure increased from 6.9 bar to 20.7 bar, and then decreased slowly with the increment of pressure, reaching 52.6 Barrer at 48 bar. In all the tests, the CH_4 permeability was in the range of 1.9~2.1 Barrer without significant change, so the trend of H_2S/CH_4 and CO_2/CH_4 separation factors was similar to the gas permeability. At 48 bar, the H_2S/CH_4 separation factor was up to 29.9, which was higher than many PI membranes [e.g., 6FDA-DAM:DABA (3:2),[39, 57] TEGMC,[56] DEGMC[56] and 6FDA-CARDO/6FDA-durene[93]] under similar conditions. The main reason for this phenomenon is the competitive sorption between H_2S and CO_2. Similar results have also been mentioned in other studies.[53, 57, 76]

Although PIM-6FDA-OH has considerable H_2S/CH_4 selectivity, the H_2S permeability of PIM-6FDA-OH was still an order of magnitude lower than that of rubbery membranes with similar H_2S/CH_4 selectivity.[108] Therefore, Yi et al.[61] functionalized PIMs with amidoxime groups. The functionalized membrane presented a lower H_2S permeability of ~4400 Barrer compared to the neat PIM-1 polymer, (~19700 Barrer) and a higher H_2S/CH_4 selectivity of ~75 (~30 for the PIM-1 precursor) with a feed pressure of 77 bar at 35 °C. On the other hand, physical aging is the main bottleneck hindering high free volume polymers from wide industrial applications.[109] In their study, the long-term stabilities of functionalized PIM membranes were continuously tested using 20/20/60% $H_2S/CO_2/CH_4$ mixture as the feed gas for 10 days with a feed pressure of 8.6 bar at 35 °C. In the first 7 days, the H_2S permeability decreased from 1391 Barrer to 867 Barrer, and then gradually stabilized. On the 10th day, it was 838 Barrer, and the H_2S/CH_4 selectivity remained at ~45. The results showed that AO-PIM-1 maintained good H_2S/CH_4 separation performance during the test without serious physical aging. Lawrence et al.[110] synthesized 10 different kinds of functionalized vinyl-added poly(norbornene) (VAPNB) (structures are showed in **Figure 10**) and studied their acid gas separation performances. In the first place, the separation

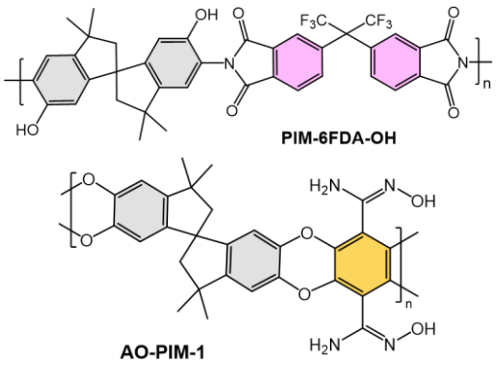

Figure 9. The molecular structure of PIM-6FDA-OH and AO-PIM-1, reproduced from ref [61, 83].

performance of 10 VAPNBs was tested in 5/3/92% $H_2S/CO_2/CH_4$ mixtures with a feed pressure of 55.16 bar at 25 °C. Among the 10 polymers, P7 showed high H_2S permeability (~3088 Barrer), the highest H_2S/CH_4 separation factor (~47.7) and the highest H_2S/CO_2 separation factor (~4.2). It's believed that the rich ether oxygen in P7 can increase the solubility of acid gas, thus improved H_2S/CH_4 separation performances.[111-113] Because of the higher H_2S solubility coefficient than CO_2, the H_2S permeability of P7 was also higher, resulting in a high H_2S/CO_2 selectivity. In addition to P7, P4 also had good H_2S/CH_4 separation performance, the H_2S permeability was up to 3475 Barrer and H_2S/CH_4 separation factor was ~26.3. The high H_2S permeability of P4 was due to the short alkyl chain of the alkoxy group in P4, which lead to the strong polarity of P4, and enhanced interaction between P4 and polar H_2S. In further gas permeation tests, 20/10/10/3/57% $H_2S/CO_2/N_2/C_2H_6/CH_4$ gas mixture was used as feed. Surprisingly, the H_2S permeability of P7 increased by 117% to 6715 Barrer, with moderate H_2S/CH_4 selectivity decrease from 47.7 to 40.5. Meanwhile, the H_2S/CO_2 selectivity of P7 was improved to 4.8. This may be due to H_2S induced plasticization under high pressure, similar to the 6FDA-based membranes. Plasticization increased the permeability of H_2S, CO_2 and CH_4, but due to competitive sorption, the solubility coefficient of H_2S in the membrane is higher than that of CO_2, which resulted in a greater proportion of H_2S permeability increase than that of CO_2, so H_2S/CO_2 selectivity increased.

PTMSP is another well-known polymer for its high free volume and consequent high gas permeability for almost all the gases. In the case of H_2S, a permeability as high as 21400 Barrer was documented, coupled with an H_2S/CO_2 ideal selectivity of 1.2, which is lower than PDMS (~1.6).[114] In another molecular dynamics simulation study, PTMSP had higher H_2S permeability, reaching 30635 Barrer, mainly due to the extremely high *FFV* and diffusivity of PTMSP.[115] However, the H_2S/CH_4 selectivity of PTMSP was only 2.28 and the H_2S/CO_2 selectivity was only 1.04. PTMSP with high gas permeability but low H_2S/CH_4 selectivity can hardly meet requirements of NG sweetening. However, it can still be applied as gutter layer or protective layer in TFC membranes.[116, 117] Non-porous PTMSP layer can prevent polymer solution from infiltrating into the porous support, which could reduce the relative resistance of TFC membranes.

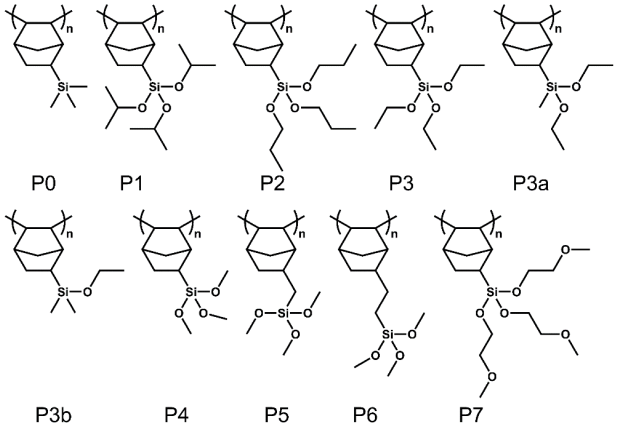

Figure 10. Molecular structures of functionalized VAPNBs, reproduced from Ref. [110]. Copyright Elsevier 2020.

According to the available data shown in **Figure 11**, PIM-based membranes show the most promising H_2S separation performance. PIM-1 demonstrated an impressive H_2S permeability of ~20000 Barrer and an H_2S/CH_4 selectivity of ~30 under an aggressive condition with feed gas containing 20% H_2S and the feed pressure as high as 77 bar.[61] Under the same condition, the H_2S permeability of AO-PIM-1 is as high as 4400 Barrer, and H_2S/CH_4 selectivity exceeds 70,[61] which is almost the highest value reported in the literature. Moreover, the H_2S separation performance of AO-PIM-1 after long-term exposure to H_2S and after regeneration is alsoattractive.[61] However, most PIM-based membranes still have similar defects as PTMSP membranes, namely significant performance loss due to severe plasticization and physical aging at high pressures and high H_2S concentrations. It is worth noting that He et al.[118] thermal annealed PIM-1 at 400 °C, and tested the annealed membranes at 35 °C and a feed pressure of 3.55 bar. The ideal CO_2/CH_4 selectivity of the obtained PIM-1-400 membrane

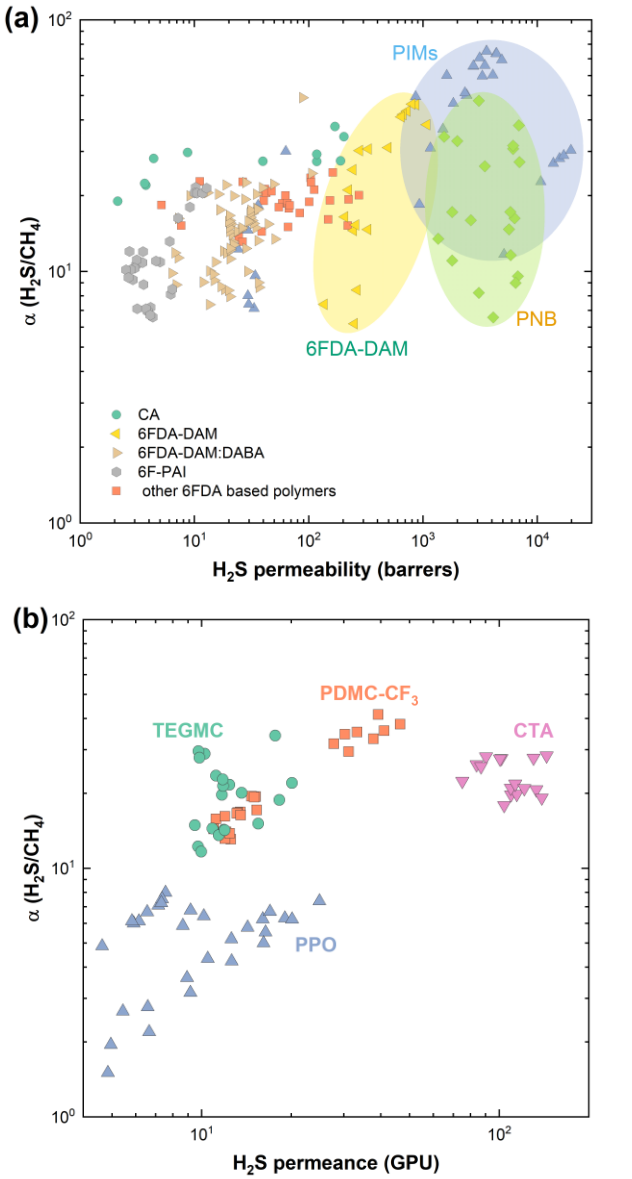

Figure 11. Comparison of H_2S separation performance of glassy polymer membranes.

increased from 15.4 to 169.5, with a CO_2 permeability up to ~228 Barrer. The thermal annealing treatment may provide options for PIM-based membranes for NG sweetening. The separation efficiency and long-term stability of PIMs and PTMSP membranes still need to be improved. CA is a widely studied and commercially used gas separation membrane material, and the H_2S permeability and H_2S/CH_4 selectivity of CA are often used as the benchmark for new gas separation membranes. In recent years, the modification of traditional CA has improved the anti-plasticization performance of CA and made it more attractive for NG sweetening under high pressure. 6FDA-based polymeri have attracted extensive research interest in recent years, -CF_3 group in 6FDA can improve the stiffness of the polymer chain and prevent polymer chains from close packing[106] so that 6FDA-based membranes often have high H_2S

permeability and H_2S/CH_4 selectivity. Unfortunately, the cost of 6FDA-based membranes is relatively high,[119] and 6FDA-based polymers undergo plasticization and physical aging,[119] which is detrimental to the long-term stability of the membranes. To sum up, in order to be able to apply the glassy polymer membranes (such as PIM- or 6FDA-based membranes) with superior H_2S separation performance in the industry, improvement of resistance to adverse plasticization at high H_2S fugacity and physical aging over long operation time may be the most critical steps. For commercialized CA membranes, improving the H_2S permeability and H_2S/CH_4 selectivity should be more important.

3.2 Rubbery Polymer Membranes

Unlike glassy polymers, the T_g of rubbery polymers is lower than room temperature or operating temperature. In general, gas permeation in rubbery polymeric membranes is mainly controlled by solubility,[87, 120] as a highly condensable gas, H_2S permeability in rubbery membranes is usually high.[121]

In 1997, Chatterjee et al.[121] synthesized two poly(ether urethanes) (named PU1 and PU3) and two poly(ether urethane ureas) (named PU2 and PU4) and used them in membranes (polymer structures are shown in **Figure 12**). First, the separation performance of $H_2S/CO_2/CH_4$ mixed gas of four polyurethane (PU) membranes at 35 °C under different H_2S contents was tested. The H_2S permeability was always much higher than CO_2 and CH_4, and H_2S/CO_2 selectivity was >3.0, due to the amino group (-NH-) in the polymer that promotes the strong interaction between H_2S and carbonyl (-C=O), making H_2S solubility much higher than other components. Among the four polymers, PU4 showed the highest H_2S/CH_4 selectivity (74), which decreased only to 66 when the H_2S content increased from 1.3% to 12.5%, which was much higher than that of CA membranes under similar conditions. Chatterjee et al. then tested the separation performance of PU4 under different H_2S content and feed pressure at 20 °C. After the temperature dropped, the permeability of H_2S, CO_2 and CH_4 decreased by about 50% but H_2S/CH_4 selectivity increased to over 93. The H_2S/CH_4 selectivity reached a maximum of 106 when H_2S content was 1.3% and feed pressure was 4.05 bar.

Sadeghi et al.[108] synthesized PU membranes with polypropylene glycol (PPG), hexamethylene diisocyanate (HDI), and 1,4-butane diol (BDO), and studied H_2S separation performance. In gas permeation tests using H_2S/CH_4 binary mixture and $H_2S/CO_2/CH_4$ ternary mixture as the feed gas, both H_2S permeability and H_2S/CH_4 selectivity increased positively with feed pressure, temperature and H_2S content increase. High pressure and high temperature enhanced the interaction between polar H_2S molecules and polar groups in PU, increasing the adsorption of H_2S, and thus increasing the H_2S permeability and the H_2S/CH_4 selectivity. Using 0.66/2.1/97.24% $H_2S/CO_2/CH_4$ ternary mixture as feed gas at 25 °C under 30 bar, H_2S permeability of 790 Barrer, H_2S/CH_4 selectivity of 27.2 and H_2S/CO_2 selectivity of 1.7 was reported for the PPG-HDI-BDO membranes.

Mohammadi et al.[122] studied the effects of feed composition, temperature and pressure on the performance of poly(ester urethane urea) (PEUU) membrane. The H_2S permeance decreased first and then rose with pressure increase. For example, in gas permeation tests using 0.6/6.2/93.2% $H_2S/CO_2/CH_4$ ternary mixture gas feed at 35 °C, it was found out that H_2S permeance rapidly decreased from 54 GPU to 38 GPU when the pressure increased from 10 bar to 20 bar, and then again increased to 48 GPU at 30 bar.

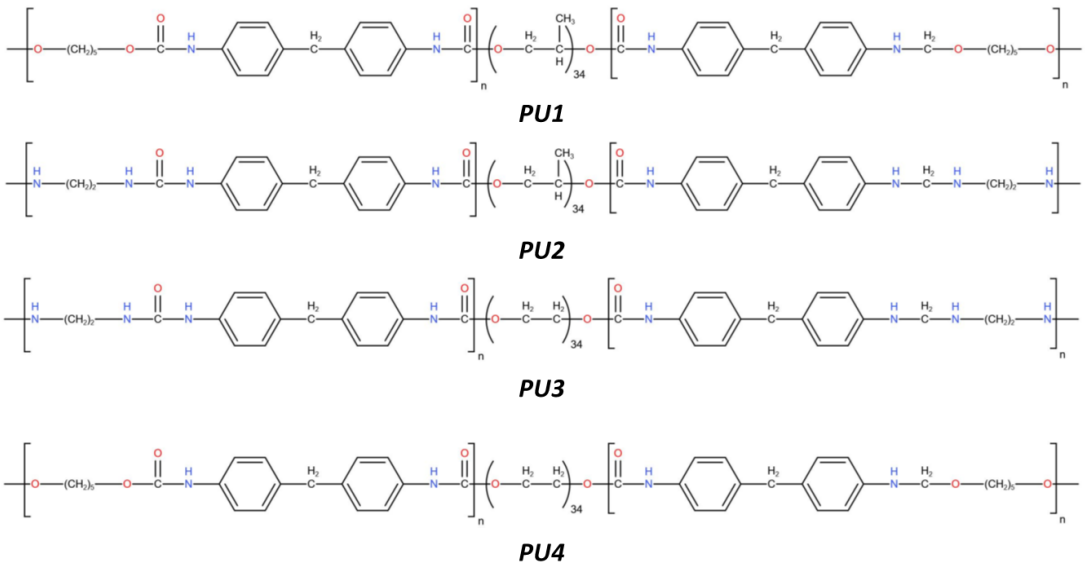

Figure 12. Molecular structures of PU1, PU2, PU3 and PU4, reproduced from Ref. [121]. Copyright Elsevier 1997.

This may be due to H_2S-induced plasticization occurred to PEUU at about 20 bar. When the temperature reached 55 °C, the trend of permeance change of various gases was more pronounced with the pressure increased.

Due to the high polarity of the polymer backbone, PEG can be used as a material to prepare membranes for H_2S/CH_4 separation.[36, 56] However, when the molecular weight is low, PEG is liquid, which is difficult to form membranes, while at too high molecular weights,

the crystalline region in PEG polymer will greatly increase, which is not permeable to the gases, thus leads to much lower gas permeability. Overall, it is difficult to use pure PEG to form membranes for gas separation.[6, 123, 124]

To develop PEG-based membranes for the simultaneous separation of H_2S and CO_2 from NG, Harrigan et al.[124] used a trifunctional isocyanate as the cross-linking agent and prepared a series of cross-linked PEG membranes. As the molecular weight of PEG increased, the T_g of polymer decreased drastically, and cross-linking had greatly reduced crystallinity. In the 5/3/92% $H_2S/CO_2/CH_4$ mixed gas permeation test, when the PEG molecular weight was less than 1000 g·mol^{-1}, it was observed that the H_2S and CO_2 permeability increased with the increase of molecular weight. When the molecular weight was 2050 g·mol^{-1}, the existence of semi-crystalline structures severely decreased H_2S, CO_2 and CH_4 permeability. When the molecular weight was 1000 g·mol^{-1}, the outstanding H_2S/CH_4 selectivity and H_2S/CO_2 selectivity was reported to be 110 and 4.9 respectively. Unfortunately, the H_2S permeability of PEG membranes was surprisingly low, for instance, the H_2S permeability of PEG with a molecular weight of 1000 g·mol^{-1} was only 26 Barrer at 55 bar. The improvement of gas permeability is essential for the cross-linked PEG membranes to be put into practical use.

Saedi et al.[125] prepared asymmetric polyethersulfone (PES) membranes via a phase inversion method,[126-128] then PDMS was coated as the selective layer on the asymmetric PES membranes. In H_2S/CH_4 binary mixture test, H_2S/CH_4 selectivity can be improved by reducing temperature, pressure and H_2S feed concentration. Similar to the phenomenon observed by Chatterjee et al.,[121] H_2S at high pressure and high feed concentration causes the PDMS layer to swell, resulting in a significant decrease in H_2S permeability and an increase in CH_4 permeability. The gas permeances in the $H_2S/CO_2/CH_4$ ternary mixture are similar to those in the binary mixture. The permeances dropped sharply with pressure increases from 10 bar to 30 bar, from 28.9 to 5.5 GPU for H_2S and from 116.1 to 9.8 GPU for CO_2. Under various test conditions, the H_2S/CO_2 selectivity was always less than 1.

Chatterjee et al.[121] compared the separation capability of seven Pebax membranes - MX 1074, MX 1657, MX 1041, 4033 SA, 3533 SA, 6333 SA and 7233 SA, for ternary mixed gases containing 1.3/27.9/70.8% $H_2S/CO_2/CH_4$ at 35 °C and 10.1 bar. Although H_2S/CH_4 selectivity of MX membranes (~50) was only about three-quarters of that of PU4 (74.0) under the same test conditions,[121] the H_2S permeability of MX 1074 was 553 Barrer, which is 2.78 times higher than PU4. When H_2S content increased to 12.5%, H_2S permeability reached 695 Barrer, which is 3.12 times higher than PU4. These separation results demonstrate that Pebax-based membranes can be applied under conditions requiring high H_2S flux.

Vaughn et al.[87] studied the separation performance of Pebax SA01 MV 3000 in single and mixed gas tests. In the single gas permeation test, H_2S permeability, H_2S/CH_4 ideal selectivity and H_2S/CO_2 ideal selectivity all increased with the increasing pressure. At 4.2 bar, the H_2S permeability was 744 Barrer, the H_2S/CH_4 ideal selectivity was 71.9 and the H_2S/CO_2 ideal selectivity was 6.6. the H_2S permeability increased to 907 Barrer at 5.5 bar. It can be seen from the single gas sorption isotherm and permeability-pressure diagram (**Figure 13**) that gas separation in Pebax mainly depended on different adsorption levels of different gas. However, a similar phenomenon wasn't observed in the mixed gas test, and instead, a significant trade-off was observed. In the gas permeation test with 20% H_2S in the feed, an H_2S permeability of 1502 Barrer and H_2S/CH_4 selectivity of 34.2 was obtained at 58.6 bar. In addition, the H_2S/CO_2 selectivity did not change with the pressure and remained at 4.3. It is worth noting that due to the fact that the poly(ethylene oxide) (PEO) blocks in Pebax MX 1657 has high affinity to acidic gases (e.g., H_2S and CO_2), thus improving the H_2S solubility and H_2S/CH_4 selectivity.[129] In fact, there are a big number of PEO-based block

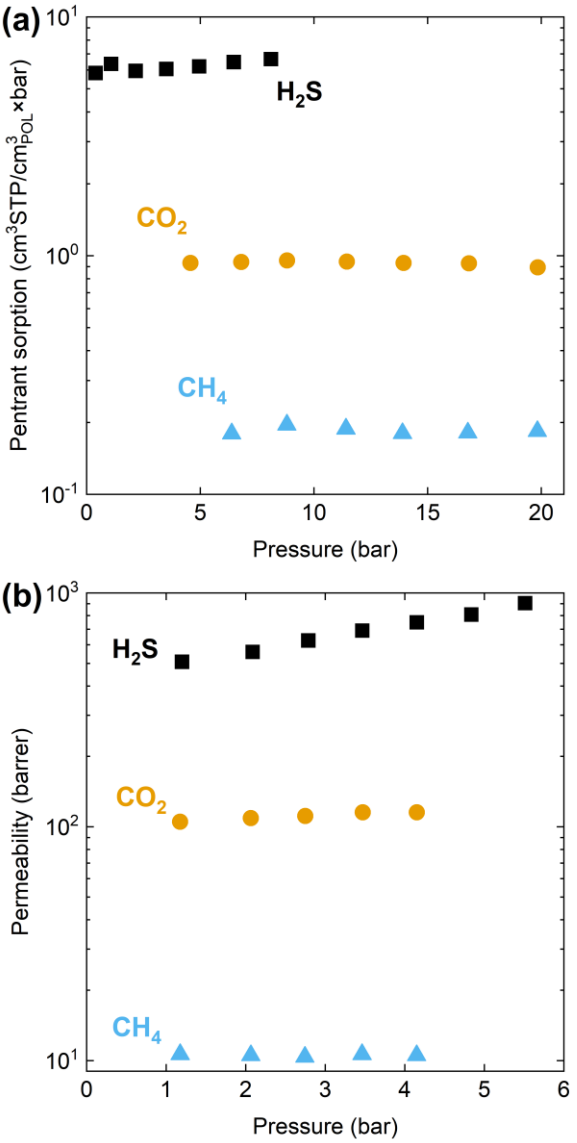

Figure 13. (a) Pure gas sorption isotherms and (b) pure gas permeabilities in Pebax SA01 MV 3000 at 35 °C. Copyright Elsevier 2014.

copolymers and cross-linked polymers, which have been widely studied for CO_2 separation and many promising results have been reported.[129-132] These PEO-based polymers are also potential materials for H_2S separation. A more detailed review of PEO-based

polymers is in the Ref.[129]. The H_2S separation performances of selected rubbery polymeric membranes are summarized in **Figure 14**. As shown in **Figure 14**, the H_2S separation performance of rubbery polymer membranes is generally better than glassy polymers. However, though rubbery polymer membranes have high H_2S permeability, they often suffer from low mechanical strength, resulting in a trade-off between permeability and mechanical stability. Traditional PU membranes can only separate H_2S at low concentrations and low pressures, which cannot meet the needs of industrial NG purification. The emerging Pebax polymers perform well at high H_2S content and higher pressure. Pebax SA01 MV 3000 exhibited high H_2S permeability (~1500 Barrer) and moderate H_2S/CO_2 selectivity (~4.3) at high pressure (55.2 bar) and high H_2S content in the feed (20% H_2S).[87] As for PEG membranes, it's necessary to find new ways to balance the mechanical and separation properties. PDMS coated PES seems to be more suitable to purify NG containing less H_2S and more CO_2. Overall, Pebax polymers are promising for natural gas purification with high H_2S content. In addition, they are already commercially available.

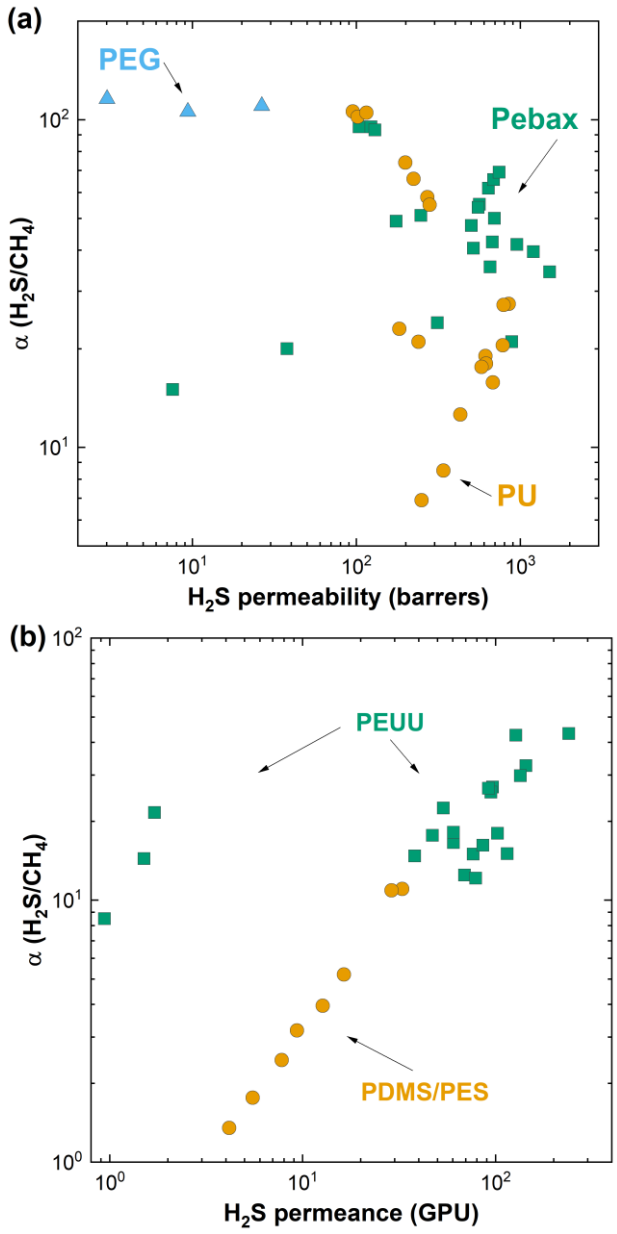

Figure 14. Comparison of H_2S separation performance of selected rubbery polymer membranes.

In the past decade, most of the research has focused on the preparation and modification of 6FDA-based PI membranes. The development trend of polymer membrane materials in the last decade is visualized in **Figure 15**. Since 2013, Koros et al.[36, 38, 39, 56, 57, 60, 86, 87] has carried out in-depth studies on 6FDA-based PI membranes for natural gas sweetening, and a series of methods including cross-linking,[56] thermal annealing[57] and PDMS post-treating[36] have been used to improve the H_2S separation properties of 6FDA-based PI membranes. In 2015, Yi et al.[83] used PI of intrinsic microporosity for the first time to separate H_2S/CH_4, and brought the separation performance of glassy polymer membranes to a new level. Since 2016, Yahaya and Bahamdan et al.[90-98] have been working on the development of novel 6FDA-based co-polymers that continuously improve the H_2S/CH_4 separation performance of membranes by changing the side chain groups of the polymer. In 2020, Lawrence et al.[110] first studied the H_2S/CH_4 separation properties of VAPNB membranes and introduced a new material for natural gas sweetening membrane. Notably, a commercially available glassy polymer, CA, has recently been shown to have excellent H_2S/CH_4 separation when slightly plasticized,[60] suggesting that plasticization may not be a "problem" for the polymers to overcome any more.[59, 60, 133] Compared with glassy polymers, rubbery polymer membranes have developed slowly in the last ten or even twenty years. The block polymers named Pebax series, commercialized in the 1980s, has overcome the trade-off between mechanical strength and H_2S separation performance of traditional PU and achieved a better H_2S/CH_4 separation efficiency.[121] Pebax has also been used in the preparation of MMMs and SILMs.[134, 135] In 2008, a commercially available PEUU HFM was shown comparable or even better performance than that of PI and CTA HFMs in the sweetening of natural gas with low sulfur content at high pressure.[122]

4 Hybrid Membranes

Polymeric membranes are well-known for good processibility and have also presented promising results for H_2S separation from NG, as shown in Figure 11 and Figure 14. Nevertheless, significant efforts have been made in exploring hybrid membranes using additive materials, such as zeolites, metal-organic frames (MOFs) and ILs, to further improve the gas separation performances. Thus, H_2S separation performances of hybrid membranes were also investigated in this work.

4.1 Mixed Matrix Membranes

Membranes with polymer as the continuous phase and inorganic additives as dispersed phase are called mixed matrix membranes

(MMMs).[136] So far, many materials have been used as fillers in MMMs, such as zeolites,[137] GO,[138] carbon molecular sieve (CMS),[139] MOFs[140] and metal nanoparticles.[141]

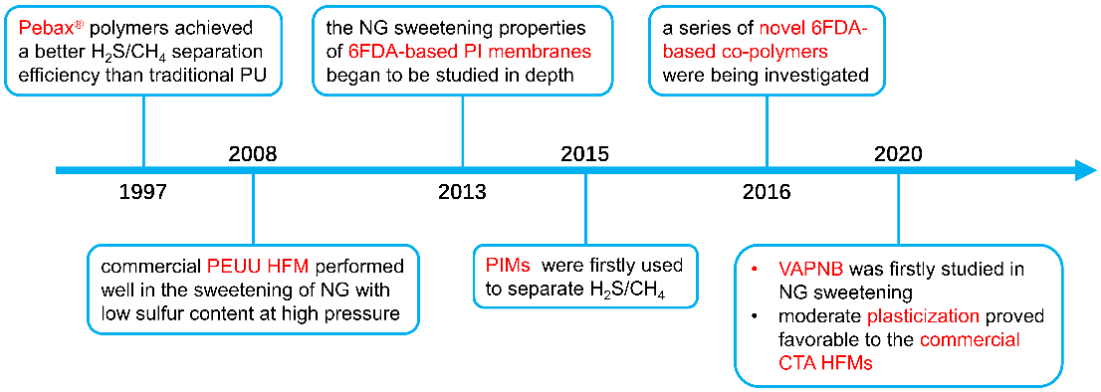

Figure 15. The timeline of development of polymeric membrane materials for natural gas sweetening over the past decade.

By introducing functional groups with strong affinity for H_2S into the ligand, such as pyridine and azole, the H_2S adsorption of MOF can be greatly improved.[142] Among different MOFs, zirconium-based MOFs represented by UiO-66 (UiO: University of Oslo) has attracted a lot of attention.[135, 140, 143, 144] UiO-66 is based on a $Zr_6O_4(OH)_4$ octahedron, it forms 12-fold lattices with 1,4-benzene-dicarboxylate (BDC) as the organic linker.[145] The theoretical specific surface area was reported to be up to 1021 $m^2 \cdot g^{-1}$.[146] Due to the crystal face-centered-cubic structure, UiO-66 has high stability towards pressure, strong acids and bases, making it suitable as a filler in MMMs for gas separation.[147]

Ahmad et al.[140] added UiO-66 and its functionalized derivatives, UiO-66-NH_2 and UiO-66-NH-$COCH_3$ into 6FDA-DAM membranes to form MMMs for H_2S separation. The separation performance of the MMMs was tested using a 5/30/65% $H_2S/CO_2/CH_4$ mixture as the feed gas, with a feed pressure of 20 bar. At 35 °C, the H_2S permeability of UiO-66-MMM was 352 Barrer, which was 2.57 times higher compared to the pure 6FDA-DAM membrane, and the H_2S/CH_4 selectivity also increased from 7.4 to 13.6. Compared with the 6FDA-DAM, the H_2S permeability of UiO-66-NH-$COCH_3$-MMM is only slightly improved and showed the highest H_2S/CH_4 selectivity (18.2) due to its reduced CH_4 permeability (from 18.5 Barrer to 10.6 Barrer). It is worth noting that exposing the MMMs to H_2S for 20~40 h has a negligible effect on both CO_2 permeability and CO_2/CH_4 selectivity, indicating that H_2S didn't induce plasticization and there was no irreversible interaction between H_2S and UiO-66.

Liu et al.[135] incorporated submicrometre-sized fillers of two rare-earth MOFs with a face-centered cubic (**fcu**) topology, Y-fumarate (*fum*)-**fcu**-MOF and Eu-1,4-naphthalenedicarboxylate (*naph*)-**fcu**-MOF, into Pebax 1074, 6FDA-DAM and 6FDA-DAM-DABA. In the single gas permeation test, the H_2S permeability and H_2S/CH_4 selectivity of all membranes increased with the content of Y-*fum*-**fcu**-MOF. In Y-*fum*-**fcu**-MOF/6FDA-DAM, the H_2S permeability increased by 110% and H_2S/CH_4 ideal selectivity increased by 35% with MOF loading increasing from 10.6 to 40 *wt*%. These experimental results are in good agreement with Liu's simulation,[135] confirming that the Y-*fum*-**fcu**-MOF can greatly improve the H_2S/CH_4 separation performance of 6FDA-DAM membranes. In contrast, the Y-*fum*-**fcu**-MOF induced H_2S/CH_4 selectivity was not significant in Pebax membranes, due to the fact that MOF reduced the mobility of flexible segments in Pebax,[148] but it enhanced the gas sorption of polymer. In the mixed gas permeation test, with the rise of pressure, both H_2S and CO_2 permeability first increased and then decreased, showing a plasticization trend similar to 6FDA-DAM. In contrast to plasticization, however, H_2S/CH_4 selectivity increased because MOF retained molecular sieve function under high pressure. In a ternary mixture permeation test with 20/20/60% $H_2S/CO_2/CH_4$ mixture as feed gas and pressure of 55 bar, the H_2S permeability, H_2S/CH_4 selectivity and H_2S/CO_2 selectivity of the 18 *wt*% Y-*fum*-**fcu**-MOF/6FDA-DAM MMMs was 956 Barrer, 33.1 and 2.0, respectively. In addition to the dense membrane, Liu et al. also prepared asymmetric HFMs with 13 *wt.*% Y-*fum*-**fcu**-MOF/6FDA-DAM as the selective layer and 6FDA-3,3',4,4'-biphenyl tetracarboxylic dianhydride (BPDA)-DAM/(P84 + SiO_2) (P84 is a brand name of polyimides manufactured by Evonik) as support. They tested the separation performance of the asymmetric HFMs for 20/20/60% $H_2S/CO_2/CH_4$ mixture at 35 °C and 6.9 bar. The obtained (H_2S+CO_2) permeation was 95 GPU, and it had an (H_2S+CO_2)/CH_4 selectivity of 43.9, which is comparable to that of flat sheet membranes (44.2).

To figure out how the fillers with finely tuned molecular transport channels improve gas separation performance of MMMs, Liu et al.[149] synthesized four fluorinated MOFs, $[Cu(SiF_6)(pyrazine)_2]_n$ (**SIFSIX**-3-Cu), $[Ni(NbOF_5)(pyrazine)_2]_n$ (**NbOFFIVE**-1-Ni), $[Ni(AlF_5)(pyrazine)_2]_n$ (**AlFFIVE**-1-Ni), and 4-cyanopyridine modified **NbOFFIVE**-1-Ni, and mixed the MOFs into 6FDA-DAM polymer. In the single gas permeation test with H_2S pressure of 1.38 bar and CH_4 pressure of 4.14 bar at 35 °C, **AlFFIVE**-1-Ni and **NbOFFIVE**-1-Ni both improved H_2S permeability and H_2S/CH_4 selectivity of the neat 6FDA-DAM membrane. **AlFFIVE**-1-Ni had a greater influence on the H_2S permeability (from 250 Barrer to 500 Barrer), while **NbOFFIVE**-1-Ni had a greater influence on the H_2S/CH_4 selectivity (from 6.2 to 9.6). It was explained by the fact that Nb^{5+} has a larger diameter than Al^{3+}, making the pore size in **NbOFFIVE**-1-Ni smaller than that in **AlFFIVE**-1-Ni. In the 20/20/60% $H_2S/CO_2/CH_4$ mixed gas

permeation test, the performance of **NbOFFIVE**-1-Ni/6FDA-DAM was better than that of Y-*fum*-**fcu**-MOF/6FDA-DAM reported by Liu.[135] At 6.9 bar, H_2S permeability of 20 *wt*% **NbOFFIVE**-1-Ni/6FDA-DAM was 401 Barrer, H_2S/CH_4 selectivity was 20.7 and H_2S/CO_2 selectivity was 0.73. The aperture size of **NbOFFIVE**-1-Ni and **AlFFIVE**-1-Ni were around 3.2 Å, so the pores could provide additional channels for acid gas molecular diffusion. Moreover, these pores acted as molecular sieves, which improved the diffusion selectivity of H_2S. In the future, accurate control of pore sizes and affinity to H_2S can provide a promising approach for the customization of fluorinated MOFs fillers for MMMs.

4.2 Ionic Liquid-based Membranes

In recent decades, ionic liquids (ILs) have been introduced as important additives in hybrid membranes for acid gas separation due to their unique properties. ILs are salts that are composed of organic cations and inorganic or organic anions. ILs hold advantages such as low vapour pressure, wide liquid temperature range, good thermal stability, good electrochemical stability and good solubility for acid gases (e.g., CO_2 and H_2S).[150, 151] **Figure 16** shows some 1-ethyl-3-methylimidazolium (EMIm)- and 1-butyl-3-methylimidazolium (BMIM)-based ILs. The solubility of H_2S in these ILs is generally much higher than that of CH_4 and CO_2,[152, 153] so these ILs are particularly suitable for H_2S separation from natural gas.

Properties of ILs can be conveniently controlled by changing the combination of anions and cations[154] so that efficient absorbents with high H_2S absorption capacity and easy regeneration can be prepared. However, the high cost and high viscosity of ILs restrict their application as gas absorbents. Combining IL with membranes can not only retain the advantage of IL's high acid gas absorption but also greatly alleviate the problem of low mass transfer efficiency caused by the large mass transfer resistance between gas and liquid phase. At present, gas separation membrane based on ILs mainly includes supported IL membranes (SILMs),[155] polymer/IL composite membranes,[156] gelled IL membranes[157] and polymerized IL membranes.[158] The disadvantages of conventional SILMs includes loss of ILs over time, narrow operational pressure differences and excessive thickness.[159] Also, the preparation of SILMs is one of the research hotspots of IL-based gas separation membranes,[155] and there are generally three methods for preparing SILMs: impregnation,[160] pressure impregnation[161] and vacuum methods.[162] Bhattacharya et al.[134] added [Emin][$EtSO_4$] IL to Pebax 2533 and tested the H_2S separation performance of hybrid membranes. Unsurprisingly, since both the solution coefficient and diffusion coefficient of H_2S in [Emin][$EtSO_4$] are greater than for CO_2,[163] the H_2S permeability also increased rapidly with the increase of ILs content. At a feed pressure of 4.9 bar and IL content of 5%, H_2S permeability and H_2S/CH_4 selectivity reached 326 Barrer and 55.9, which were 3.2 and 2.5 times higher compared to pure Pebax (P_{H_2S} =102 Barrer, α_{H_2S/CH_4} =22.6), respectively. Meanwhile, CO_2 permeability was 38 Barrer and H_2S/CO_2 selectivity was 8.6. The effect of feed pressure on the hybrid membrane with 5% ILs showed that with pressure rise in the range of 2.9~6.9 bar, the H_2S, CO_2 permeability, and H_2S/CH_4, CO_2/CH_4 selectivity all increased. At 6.9 bar, the H_2S permeability was 540 Barrer, the H_2S/CH_4 selectivity was 66, and the H_2S/CO_2 selectivity reached a surprisingly high value of 9.8. The [Emin][$EtSO_4$]/Pebax 2533 MMM provided excellent performance for separating H_2S, however, long-term stability tests under higher pressure are needed.

Park et al.[159] studied the effects of different preparation and operation parameters on single gas permeability of SILMs based on [Bmim][BF_4]. With the IL content increased from 0.5 to 2.0 *wt*.%, the permeability of H_2S increased sharply from ~160 Barrer to ~960 Barrer, and the H_2S/CH_4 selectivity increased from ~170 to ~215 (IL content of 1.5) and then decreased to ~195. The addition of IL decreased the crystallinity and *FFV* of the membrane and increased the diffusion coefficient, leading to the decrease of selectivity. The permeability of all gases increased with the increase of operating temperature, but the selectivity decreased. With the increase of temperature, the viscosity of IL decreases sharply[162] and the intermolecular interactions weaken, leading to the reduction of the acid gas absorption.

Zhang et al.[160] selected five kinds of ILs, namely, [Bmim][Ac], [Bmim][PF_6], [Bmim][CF_3SO_3], [Bmim][BF_4] and [Bmim][Tf_2N], to prepare SILMs. In SILMs with [Bmim][PF_6], [Bmim][CF_3SO_3], [Bmim][BF_4] and [Bmim][Tf_2N], the permeability of H_2S increases with the increase of alkalinity of the ILs,[164] and when in the membrane based on [Bmim][Ac], H_2S can be complexed with IL to form 2[Bmim][Ac]·H_2S complex,[165] leading to a much higher H_2S permeability of (7304 Barrer), which is about 1.70 ~ 3.83 times higher compared to the other four SILMs. It was also observed for the first time that the permeability of H_2S in [Bmim][Ac] decreased with the increase of transmembrane pressure, which fully indicated that the [Bmim][Ac] immobilized SILMs are facilitated transport membranes.[166] Since there is no interaction between CH_4 and IL, the permeability of CH_4 is negatively correlated with the viscosity of IL[152, 165, 167-173] and the difference is very small, so that [Bmim][Ac] with the highest H_2S permeability has also the highest H_2S/CH_4 ideal selectivity (136), which is 2.68 ~ 6.87 times higher than that of other SILMs. Besides, although [Bmim][CF_3SO_3] and [Bmim][BF_4] also have high H_2S permeability (4303 Barrer and 4059 Barrer, respectively) and H_2S/CH_4 selectivity (50.7 and 36.6, respectively), in the theoretical calculation, the H_2S/CO_2 selectivity is too poor to realize the selective separation of H_2S and CO_2, which may be due to the competitive absorption between CO_2 and H_2S in these ILs.[162] As a result, the [Bmim][Ac] with high H_2S permeability, high H_2S/CH_4 selectivity and high H_2S/CO_2 selectivity (11.7) could have a great potential for selective separation of H_2S from CO_2 and CH_4.

Akhmetshina et al.[162] prepared [Bmim][BF_4] and [Bmim][OAc] immobilized SILMs with hydrophobic tetrafluoroethylene-vinylidene fluoride copolymers (MFFK-1) as support. All the gas separation tests were carried out at a feed pressure of 2 bar. As mentioned above, the [Bmim][OAc] immobilized SILMs are facilitated transport membranes, and the gas permeability decreases with the increase of pressure.[166] Therefore, the gas permeabilities of single component H_2S in this study are far lower than that in Zhang et al. (permeation test carried out at 0.1 bar).[160] During the preparation of [Bmim][BF_4], it was also found that

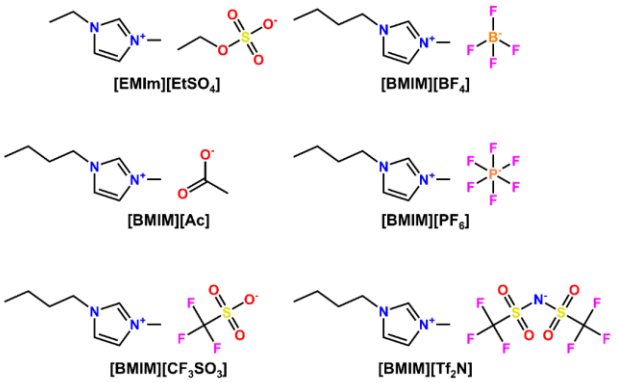

Figure 16. Structures of commonly used ILs in SILMs for H_2S separation.

impurities (e.g. H_2O) in the ILs will have negative effects on the solubility of both CO_2 and H_2S in ILs.[174] Mixed gas permeation tests were also carried out with 5/15/85% $H_2S/CO_2/CH_4$ mixture as feed for the first time.[162] [Bmim][BF_4] showed slightly higher H_2S gas permeability (142 Barrer), but the H_2S/CH_4 selectivity (16.4) was much lower than that of [Bmim][OAc] (106.2). This could be explained by the extremely low CH_4 solubility in [Bmim][OAc][175] and a consequent low CH_4 permeability in [Bmim][OAc] (~1 Barrer). When considering the competitive sorption between H_2S and CO_2 in ILs, the H_2S/CO_2 selectivity of [Bmim][BF_4] (2.05) is almost twice that of [Bmim][OAc] (1.10).

Up to now, there are few studies on the separation of H_2S/CH_4 and $H_2S/CO_2/CH_4$ with SILMs. Similar to SILMs for CO_2/CH_4 separation, further improvements to SILMs for H_2S/CH_4 separation are needed before they can be scaled up to an industrial scale. Although [Bmim][Ac] based SILMs have shown excellent H_2S/CH_4 separation performance, severe ILs loss may occur under high pressure. Therefore, it's necessary to develop SILMs with good stability and H_2S separation performance under high pressure. More than that, as mentioned before, most of the existing SILMs are facing the problems of excessive thickness and a narrow range of operating temperature,[176] which seriously limits the potential of their application.

From **Figure 17**, it is seen that the H_2S separation performance of the hybrid membranes, especially the SILMs, is much better than that of the polymer membranes. However, the preparation cost of hybrid membranes is often much higher than that of polymer membranes. From the point of view of the preparation of MMMs, it is very important to evenly disperse functional fillers in the membrane. The agglomerated nanoparticles will produce more non-selective voids, thus reducing the selectivity of the MMMs. The commonly used methods for uniform dispersion of fillers are to prepare monodisperse fillers and to increase the compatibility between fillers and polymer matrix.[177] Compared to other nanofillers employed in MMMs, it is relatively easy to improve the compatibility between MOFs and polymer matrix, or increase the

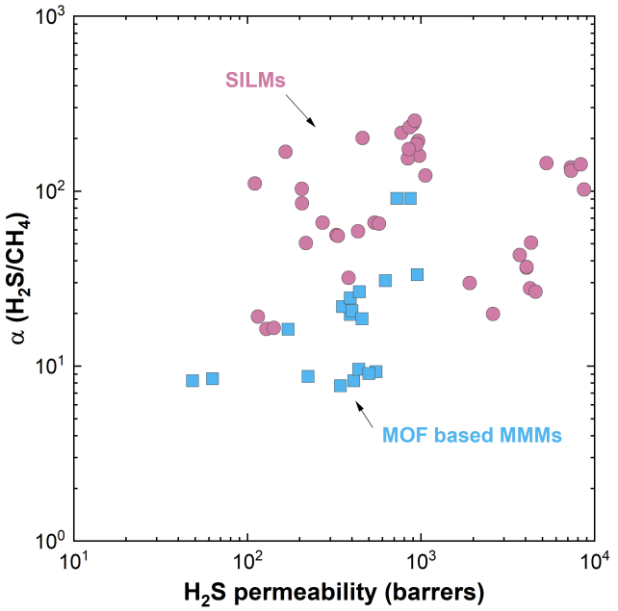

Figure 17. Comparison of H_2S separation performance of hybrid membranes.

repulsive force between MOF particles by changing the type of organic ligand.[178] Therefore, the MMMs with MOFs as filler can be a promising hybrid membranes for NG sweetening. Moreover, some problems may arise during the operation of the hybrid membranes, such as interface inconsistency between polymer matrix and fillers caused by plasticization of glassy polymers under high pressure, or the loss of ILs in the SILMs due to excessive operating pressure. Therefore, in addition to the H_2S permeability and H_2S/CH_4 selectivity improvement of hybrid membranes, it is necessary to continuously improve the long-term stability in actual operating conditions. Mozafari et al.[179] used porous polymethylpentene (PMP) as the carrier, immersed the carrier in Pebax solution with dispersed nano-MOF particles, and then evaporated the solvent to obtain the TFNM with micron-sized selective layer. This preparation process reduces the amount of MOF and results in excellent separation CO_2/CH_4 separation performance, exceeding the 2008 Robeson upper bound. The similar idea can also be applied to natural gas sweetening. By changing the combination of polymer and filler, it is possible to obtain TFNMs with both high H_2S permeability and high H_2S/CH_4 selectivity. Besides, the preparation cost and operation cost of the hybrid membranes should be also taken into account.

5 Membrane Contactors

Membrane contactor is attracting more and more attention for acid gas separation in recent years. Membrane contactor combines the advantages of traditional liquid absorption, *i.e.,* high selectivity, high tolerance to impurities, and the advantages of membrane separation, such as high operational flexibility, small footprint and linear scalability.[180, 181] In addition, membrane contactors do not encounter the mass transfer efficiency reduction caused by flooding, foaming or entrainment as in a traditional packed tower.[182] **Figure 18** shows the process of NG purification using membrane contactors.

Normally, the NG and the liquid absorbents undergo counter-flow on two sides of the membrane. Typically, only the porous membranes are used in membrane contactors thus they have no selectivity. The solubility difference of various gases in the absorbents provides selectivity for the membrane contactor.[183]

These unique advantages of membrane contactors have attracted researchers to explore their application in the field of NG separation and purification.[184-191] The main research directions include the selection of membrane materials and absorbent, mathematical simulation of mass transfer process and optimization of operating conditions.

Polytetrafluoroethylene (PTFE) and polyvinylidene fluoride (PVDF) are often used as membrane materials in membrane contactors due to their hydrophobicity.[192] However, PTFE and PVDF still undergo membrane wetting under high pressure. Once the absorbent enters into the pores, it will greatly increase the mass transfer resistance and decrease of H_2S permeation flux.[193-196] Abdolahi-Mansoorkhani et al.[197] proposed to load $CaCO_3$ nanoparticles on the PVDF surface to improve the H_2S removal rate by improving surface roughness and increasing the contact area between the membrane and gas. It was shown through mathematical modeling, that the H_2S removal rate of 20 *wt*% $CaCO_3$ nanoparticles loaded PVDF increased from 73% to 82%, compared with pure PVDF under the same conditions. Similarly, Li et al.[193] prepared the ultra-hydrophobic HFM by spray-deposing SiO_2 nanoparticles on PTFE membranes. The experimental

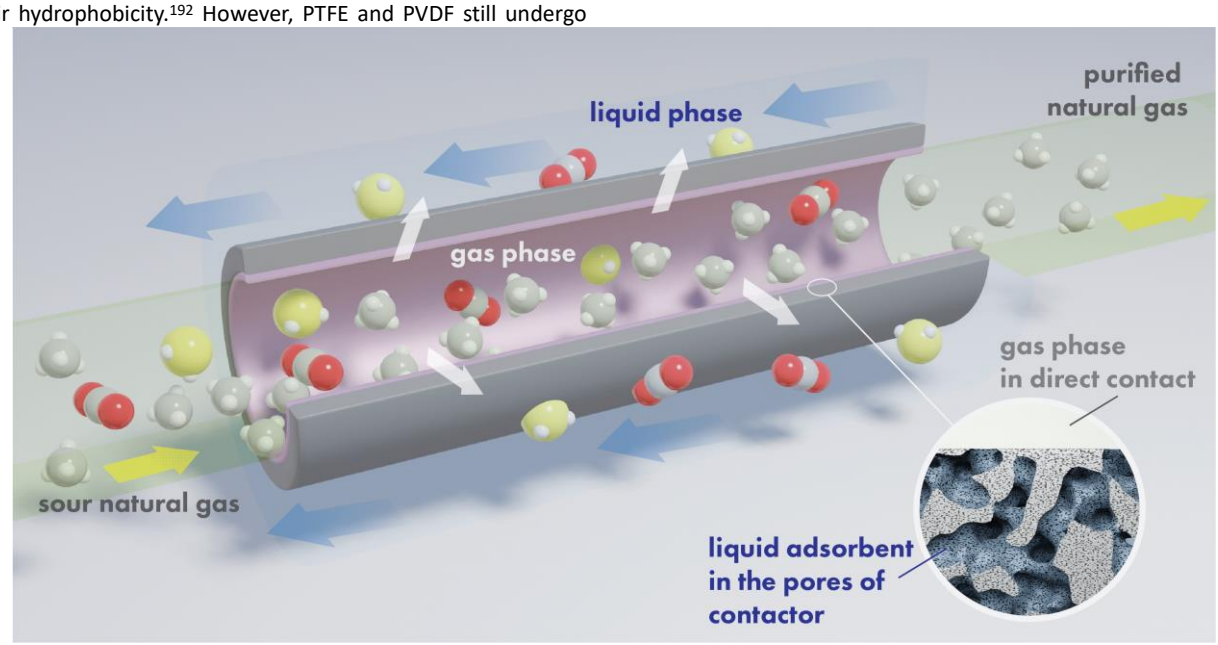

Figure 18. Schematic diagram of the working principle of membrane contactor.

results showed that SiO_2 nanoparticles can prevent membrane wetting under high pressure. In addition to nanoparticles, Lv et al.[198] deposited a mixture of cyclohexanone and methyl ethyl ketone (MEK) on PP to improve its hydrophobicity. However, the deposition would reduce the surface porosity and increase the membrane thickness, resulting in a higher mass transfer resistance. Tilahun et al.[199] attempted to directly prepare HFM with PDMS, and its intrinsic selectivity reduced the methane loss to a certain extent.

Common absorbents can be divided into physical and chemical types. Physical absorbents include water and ILs, and chemical absorbents include K_2CO_3, MEA, DEA, TEA, MDEA, etc. Hedayat et al.[200] used MEA/MDEA mixed solution as absorbent and obtained good H_2S removal efficiency. The reaction rate of alkanolamine with H_2S is fast, but alkanolamine is corrosive and has low surface tension.[201] NaOH solution is also an attractive absorbent because it has a relatively high volumetric liquid side mass transfer coefficient, but it will react with H_2S and CO_2 to form salts, thus reducing the absorption rate.[202] To replace NaOH, K_2CO_3 was employed as the absorbent. Although it has slower reaction kinetics, its high stability, low price and environmental friendliness make it competitive.[203] Some studies have shown that solutions of amino acid salts, such as potassium lysinate and potassium L-arginine, are promising absorbents.[190, 204] There may be an interaction between potassium lysinate and K_2CO_3, which is conducive to the absorption of H_2S and CO_2, while potassium L-arginine itself absorbs H_2S and CO_2 more efficiently than MEA. However, the high cost of preparing and recycling amino acid salts limits its application.

A large number of studies have been conducted on the effects of operating parameters on the separation performance of membrane contactor. These studies mainly focus on gas/liquid velocity, operating pressure, absorbent concentration and inlet composition. **Table 4** lists operating parameters and H_2S removal performance of selected hollow fiber membrane contactors (HFMCs) for NG sweetening.

Gas velocity is considered to have a great influence on H_2S removal.[197, 205] Even though a higher gas velocity results in a higher mass transfer coefficient, a lower gas velocity means a longer residual time in the HFM, thus resulted in a higher H_2S removal rate. And if gas velocity cannot be slowed, it may be a good choice to increase the packing density of HFM in the membrane module to

lower the gas-liquid ratio.[188, 206] The influence of liquid velocity on H_2S removal rate is not as great as that of gas velocity. When the liquid velocity increases, the gas concentration at the gas-liquid contact surface can be diluted faster and gas absorption can be promoted.[206, 207] In the same way, the gas and liquid phases flow in opposite directions can also improve the separation efficiency of H_2S, too.[197] Increased operating pressure is generally favorable for H_2S separation because it increases the gas solubility of H_2S in the liquid phase, meanwhile slightly increased the mass transfer coefficient.[200, 207]

In most membrane contactors using alkanolamine and alkali solution as absorbent, the removal rate of H_2S is positively correlated with the absorbent concentration.[197, 199, 200, 208] It is noteworthy that Faiz et al.[209, 210] reported the effect of carbonate concentration on H_2S absorption rate. With inlet CO_3^{2-} concentration increased from 0 to 2 mol/L, the removal rate of H_2S first increased and then decreased, and it reached the highest removal rate of 63% when inlet CO_3^{2-} concentration was about 1 mol/L. It is believed that due to the salting-out effect, H_2S solubility will decrease when the CO_3^{2-} concentration increases. Moreover, there will be large amounts of HCO_3^- in the liquid phase with continuous feeding, which will move the equilibrium toward the formation of H_2S, thereby inhibiting the dissolution of H_2S in the absorbent. Therefore, Faiz proposed that two membrane module can be connected in series. In the first module, the liquid phase flow rate should be increased to remove as much H_2S and CO_2 as possible. For the second module, fresh absorbent will be used to completely remove the acid gas. As Tantikhajorngosol et al.[211] suggested, the multistage module is beneficial to improve the H_2S removal rate. In

Table 4. Gas-liquid phase, working conditions and efficiency of various membrane contactors.

Membrane	Liquid phase	Gas phase ($H_2S/CO_2/CH_4$)	Pressure (bar)	H_2S removal efficiency (%)	CO_2 removal efficiency (%)	Ref.
ePTFE	water	2/5/93	50	82	60	[184]
	water	2/5/93	50	77	55	
	water	2/5/93	50	70	49	
	0.1 M NaOH	2/5/93	50	90	88	
	2.0 M NaOH	2/5/93	50	99	100	
	0.5 M MEA	2/5/93	50	96	98	
	0.5 M DEA	2/5/93	50	94	91	
	0.5 M DETA	2/5/93	50	98	97	
PFA	water	2/5/93	50	85	52	
	water	2/5/93	50	83	44	
	water	2/5/93	50	76	43	
	0.1 M NaOH	2/5/93	50	94	48	
	2.0 M NaOH	2/5/93	50	100	100	
	0.5 M MEA	2/5/93	50	100	94	
	0.5 M DEA	2/5/93	50	100	84	
	0.5 M DETA	2/5/93	50	100	98	
ePTFE	water	2/0/98	50	100	N.A.	[185]
	water	2/0/98	50	93	N.A.	
	water	2/0/98	50	83	N.A.	
	water	2/0/98	50	74	N.A.	
	water	2/0/98	50	56	N.A.	
	water	2/0/98	50	80	N.A.	
	0.1 M NaOH	2/0/98	50	90	N.A.	
	0.5 M NaOH	2/0/98	50	96	N.A.	
	2.0 M NaOH	2/0/98	50	100	N.A.	
	0.1 M MEA	2/0/98	50	91	N.A.	
	0.5 M MEA	2/0/98	50	97	N.A.	
	2.0 M MEA	2/0/98	50	100	N.A.	
	0.5 M DEA	2/0/98	50	85	N.A.	
	0.5 M TETA	2/0/98	50	97	N.A.	
ePTFE	water	2/0/98	1	29	N.A.	[186]
	water	2/0/98	1	19	N.A.	
	water	2/0/98	1	15	N.A.	
	water	2/0/98	1	14	N.A.	
	water	2/0/98	10	70	N.A.	
	water	2/0/98	10	54	N.A.	
	water	2/0/98	10	44	N.A.	
	water	2/0/98	10	36	N.A.	

	water	2/0/98	20	91	N.A.	
	water	2/0/98	20	76	N.A.	
	water	2/0/98	20	63	N.A.	
	water	2/0/98	20	52	N.A.	
	water	2/0/98	30	75	N.A.	
	water	2/0/98	40	80	N.A.	
	water	2/0/98	50	83	N.A.	
PVDF	water	0.05/40/59.95	30	61	41	[187]
PTFE	water	0.05/40/59.95	30	58	46	
PFA	water	2/5/93	50	48.5	28	[188]
	0.5 M K_2CO_3	2/5/93	50	99	73	
	2.0 M K_2CO_3	2/5/93	50	99.4	68	
	1.5 M K_2CO_3 +0.5 M $KHCO_3$	2/5/93	50	96.4	48.6	
	1.0 M K_2CO_3 + 1.0 M $KHCO_3$	2/5/93	50	96.1	47	
	0.5 M K_2CO_3 + 1.5 M $KHCO_3$	2/5/93	50	95.7	43	
PVDF	water	0.05/40/59.95	N.A.	24	5.3	[189]
	0.5 M MEA	0.05/40/59.95	N.A.	75	53	
	0.125 M MEA	0.05/40/59.95	N.A.	57	13	
	0.125 M MEA	0.05/40/59.95	N.A.	60	15	
	0.5 M MEA	0.05/40/59.95	N.A.	69	44	
	0.5 M MEA	0.05/40/59.95	N.A.	71	49	
	1 M MEA	0.05/40/59.95	N.A.	73	72	
	1 M MEA	0.05/40/59.95	N.A.	78	83	
	0.5 M MEA	0.05/40/59.95	N.A.	73	62	
	0.5 M MEA	0.05/40/59.95	N.A.	61	44	
PFA	0.5 M K_2CO_3	2/5/93	N.A.	100	45	[190]
	0.5 M K_2CO_3	2/5/93	N.A.	95	45	
	0.5 M (K_2CO_3 + PL)	2/5/93	N.A.	100	99	
	0.5 M (K_2CO_3 + PL)	2/5/93	N.A.	98	94	
PP	0.5 M MDEA	0.5/4/95.5	1.5	100	100	[191]
	0.5 M MDEA	2.5/4/93.5	1.5	97	68	
	0.5 M MDEA	0.5/4/95.5	1.5	99	99	
	0.5 M MDEA	2.5/4/93.5	1.5	98.5	44	
	0.5 M MDEA	1.5/4/94.5	1.5	100	100	
	0.5 M MDEA	1.5/20/78.5	1.5	100	64	
	0.5 M MDEA	1.5/4/94.5	1.5	100	50	
	0.5 M MDEA	1.5/20/78.5	1.5	100	19	

addition, for economic reasons, Esquiroz-Molina[208] recommends an optimal pH of about 11 when using NaOH as the absorbent to remove H_2S and CO_2 from NG. When MDEA was used as the absorbent, the CO_2 concentration had little influence on the H_2S removal rate, and the H_2S/CO_2 selectivity had been maintained between 25 and 50.[191] That was because that H_2S reacts with MDEA at a much faster rate than CO_2.[207]

In addition to membrane material, absorbent species, gas velocity and operating pressure, the effects of temperature,[188, 197, 200] membrane tortuosity[205] and membrane wetting ratio[212] on the performance of membrane contactor have been explored through modeling. It is found out that high temperature increases gas flux and H_2S removal rate.[188, 197] The mass transfer resistance of the membrane increases with the increase of the membrane curvature, leading to a significant decrease in both mass transfer and removal rate of H_2S.[205] When the membrane is wetting, the pores in the membranes are partially or completely filled with absorbent, which leads to the increase of gas mass transfer resistance and the higher the wetting ratio, the lower the absorption rate of H_2S.[212] A series of recent studies have shown that membranes with a dense skin layer on the surface can effectively avoid the problem of membrane wetting.[196, 213-215] Though the dense structure inevitably increases the mass transfer resistance of gas through the membranes, it provides a promising method for the application of membrane contactors at high pressure.

The operating unit of membrane contactor is more complex than that of gas separation membranes so that more factors are affecting the performance of membrane contactors. In addition to the combination of membrane material and liquid absorbent, operating conditions such as gas and liquid velocity, pressure and temperature, and subsequent conditions for absorbent regeneration should be taken into consideration in the research scope. In future research, it's also of great value to carry out the techno-economic analysis and life cycle analysis on the existing membrane contactors.

6 H_2S separation performances comparison

In **Table S1** and **Table S2**, the H_2S separation performance and corresponding test conditions (feed gas content, temperature and feed pressure) of different membranes are respectively sorted out. Up to 104 different membrane materials and more subtle differences between various membranes under similar test conditions can be seen in the detailed data. For the convenience of the readers, the H_2S separation performances of various membranes and membrane processes were summarized in **Figure 19.** In addition, the H_2S/CH_4 upper bound was fitted using the standard equation $P = k\alpha^n$ (where P is permeability (Barrer) of the more permeable H_2S gas, k is the front factor (Barrer), α is the selectivity for H_2S/CH_4 gas pair, and n is the slope. The *n* and *k* values for H_2S/CH_4 gas pair are given in **Table 5**. Compared to the value proposed by George et al. in 2016, it is found out there has been certain progress in polymeric membranes, thus leading to different *n* and *k* values (presented in **Table 5**). In addition, if nanofillers or liquids are included in the comparison, the obtained distribution for hybrid membranes present much better H_2S/CH_4 separation performances (green triangle data points in **Figure 19**), thus a new upper bound was also proposed for hybrid membranes(presented in **Table 5**). It is worth mentioning that the flux values obtained in membrane contactors were also converted into permeance, to compare with conventional membrane gas separation processes.

As can be seen from **Figure 19(a)**, higher H_2S permeability are normally obtained for glassy polymers, while rubbery polymers often show higher H_2S/CH_4 selectivity. Overall, it seems hybrid membranes are promising for H_2S separation applications as they combine the advantages of both polymeric and inorganic membrane materials. When comparing the H_2S permeance, as shown in **Figure 19(b)**, not surprisingly, glassy and rubbery polymers exhibit rather similar H_2S selectivity. Rubbery polymers show slightly higher H_2S permeance. However, glassy polymers usually present better mechanical stability, and also compared to rubbery polymers, there are more glassy polymer candidates to be applied for H_2S separations. It is worth mentioning that membrane contactor has been also studied for H_2S separation. Compared with conventional gas separation processes, membrane contactor (the data was obtained from Ref. [187]) shows relatively high H_2S/CH_4 selectivity, but far lower H_2S permeance than many polymeric membranes, thus making membrane contactors not that promising for H_2S removal from NGs.

7 Conclusions and perspectives

Natural gas sweetening using membrane technology holds the advantages of simple operation, small footprint, no secondary pollutions, etc. In most literature, most studies in NG treatment was dedicated to CO_2/CH_4 separation. In the past few years, research has also been carried out on H_2S removal from NG. In the current work, various membranes applied for H_2S separation were systematically summarized and discussed, including neat glassy/rubbery polymer membranes, hybrid membranes and membrane contactors.

For glassy membranes, series of new materials with high H_2S and H_2S/CH_4 selectivity have been developed, such as the 6FDA-based PIs and functionalized PIMs [e.g., AO-PIM-1 has extremely high H_2S permeability (>2000 Barrer) and H_2S/CH_4 selectivity (>50)]. Nevertheless, the problem of H_2S induced plasticization and physical aging need to be solved for most glassy polymeric membranes before application. At the same time, while trying to improve the H_2S separation performance, more experiments should be carried out to investigate the membrane durability in the presence of H_2S, which is an important factor to evaluate the practicability of membranes. Meanwhile, it is important to note that for different types of membranes, varying degrees of plasticization are not always harmful. More in-depth study is needed to understand the specific effect of H_2S on membrane plasticization and physical aging. A variety of methods have been developed, such as cross-linking, adding nanofillers, and even thermal regeneration. However, most of those strategies need to be further studied before they could be applied in industrial applications.

On the other hand, rubbery membranes present relatively higher H_2S permeability and H_2S/CO_2 selectivity compared to glassy polymer, but there exists a performance-mechanical property balance, efforts dedicated to improving the segment flexibility often results in the loss of the mechanical properties, which limits the application of rubbery membranes. Attempts have been made to improve the mechanical properties by employing cross-linking, or coating rubbery polymer onto porous supports, which were proven not that efficient. Developing block-copolymers with both hard segments offering mechanical strength and soft part for high H_2S affinity can be a promising option.

Table 5. The *n* (slopes) and *k* (front factors) for H_2S/CH_4 gas pair.

k (Barrer)	n	Ref.
2.10×10^7	-2.43	2016 (George et al.[6])
4.20×10^{21}	-9.60	2021 (polymeric membranes)
1.81×10^{12}	-3.83	2021 (for hybrid membranes)

Combining polymeric membrane with (in)organic filler is another intensively investigated strategy to improve gas separation performances. Good H_2S separation performance was achieved for a number of hybrid membranes due to the addition of fillers which are beneficial to H_2S permeation or H_2S/CH_4 separation. In addition, compared with the neat polymeric membranes, some of the MMMs with MOFs as the filler has better physical aging resistance and can maintain high H_2S permeability. On the other hand, supported ionic

liquid membranes, is also studied for H_2S separation from NGs, similar to other applications of SILMs, brilliant results can be obtained in the lab with moderate test conditions and in a short testing period, applying SILMs in harsh conditions (e.g., high feed pressure, the high water content in the feed) and maintaining its long-term stability is still challenging.

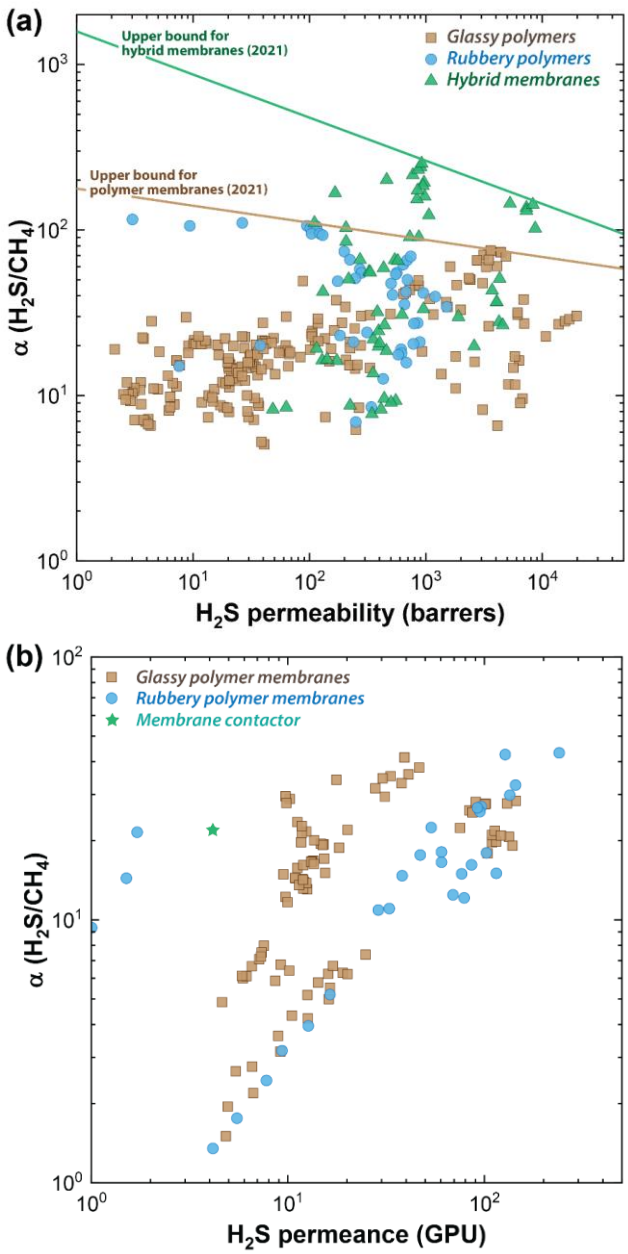

Figure 19. (a) State of the art H_2S/CH_4 separation performance for the glassy polymer, rubbery polymer and hybrid membranes with suggested updated upper bounds; (b) H_2S/CH_4 selectivity vs. permeance for the membranes made of glassy and rubbery polymers compared to the estimated value for the membrane contactor.[187]

Membrane contactors have been also studied for removing H_2S from NGs. In many cases, due to the low H_2S content in the NGs, the membrane contactors were used to simultaneously remove CO_2 and H_2S. So far, there are only a few research works on the sweetening of high sulfur natural gas by using membrane contactors. In most studies, due to low H_2S content (usually <1%) in the feed gas, after converting the H_2S flux to H_2S permeance, H_2S separation performances of the membrane contactors are not competitive compared to conventional polymeric membranes.

Based on the conclusions of our study, some perspectives of future research were also proposed:

(1) For glassy polymeric membranes, introducing bucky side groups into the polymeric chain to improve the free volume and hence to increase the H_2S diffusivity can be one option. Introducing partially cross-linked structures into the polymeric matrix to enhance the rigidity, thus improve the plasticization resistance, can be another. Thirdly, introducing specific functional groups with a strong interaction with H_2S (such as CF_3) into the polymer structure to improve H_2S solubility can also be an option.

(2) For rubbery membranes, developing new rubbery materials to balance the mechanical stability and separation performances is the critical step for applying rubbery membranes in H_2S separation. Facile thin-film-composite membrane fabrication of rubbery polymers with low mechanical strength but high H_2S separation performance should be an important research direction.

(3) For hybrid membranes, reducing the non-selective gap between fillers and polymer matrices, avoiding blocking the filler's micropores, and preventing polymer chain migration caused by the fillers should be the focuses in the future development of MMMs. Computational and mathematical models can also be used to predict the optimal shape and structure of the fillers in the polymer matrix and to suggest the appropriate loading amount in advance, with further exploration of the specific impact of the fillers on H_2S diffusion and solution in the MMMs through experiments.

(4) In the case of membrane contactors, as the NG sweetening process is almost always carried out at high pressures, how to maintain the long-term stability of membrane contactors is of critical importance. In addition, developing new absorbents for simultaneously removing CO_2 and H_2S from NG is interesting. Strategies to reuse or resource the separated CO_2 and H_2S can be another interesting topic.

Conflicts of interest

There are no conflicts to declare.

Acknowledgements

This work is supported by the National Key R&D Program of China (2019YFC1906700) and Sichuan Science and Technology Program (2021YFH0116).

References

1 S. Faramawy, T. Zaki and A. A. E. Sakr, *J. Nat. Gas Sci. Eng.*, 2016, **34**, 34-54.
2 B. Zeng and C. Li, *Energy*, 2016, **112**, 810-825.
3 Carbon Dioxide Emissions Coefficients, https://www.eia.gov/environment/emissions/co2_vol_mass.php, (accessed 29 May 2021).
4 *Statistical Review of World Energy 2020*, BP p.l.C., London, United Kingdom, 2020.
5 *International Energy Outlook 2019*, U.S. Energy Information Administration, Washington, DC, 2019.
6 G. George, N. Bhoria, S. AlHallaq, A. Abdala and V. Mittal, *Sep. Purif. Technol.*, 2016, **158**, 333-356.
7 B. D. Bhide, A. Voskericyan and S. A. Stern, *J. Membr. Sci.*, 1998, **140**, 27-49.
8 L. Peters, A. Hussain, M. Follmann, T. Melin and M. B. Hägg, *Chem. Eng. J.*, 2011, **172**, 952-960.
9 J. Wang, Z. Song, H. Cheng, L. Chen, L. Deng and Z. Qi, *Sep. Purif. Technol.*, 2020, **248**, 117053.
10 M. S. Shah, M. Tsapatsis and J. I. Siepmann, *Chem. Rev.*, 2017, **117**, 9755-9803.
11 Energy Outlook, https://www.bp.com/en/global/corporate/energy-economics/energy-outlook/demand-by-fuel/natural-gas.html, (accessed 29 May 2021).
12 O. W. Awe, Y. Zhao, A. Nzihou, D. P. Minh and N. Lyczko, *Waste Biomass Valorization*, 2017, **8**, 267-283.
13 R. W. Baker and K. Lokhandwala, *Industrial & Engineering Chemistry Research*, 2008, **47**, 2109-2121.
14 A. Tabe-Mohammadi, *Sep. Sci. Technol.*, 1999, **34**, 2095-2111.
15 J. Li, Z. Xie, J. Dai, S. Zhang, G. Zhu and Z. Liu, *Org. Geochem.*, 2005, **36**, 1703-1716.
16 G. Zhu, S. Zhang, H. Huang, Y. Liang, S. Meng and Y. Li, *Applied Geochemistry*, 2011, **26**, 1261-1273.
17 M. W. Seo, Y. M. Yun, W. C. Cho, H. W. Ra, S. J. Yoon, J. G. Lee, Y. K. Kim, J. H. Kim, S. H. Lee, W. H. Eom, U. D. Lee and S. B. Lee, *Energy*, 2014, **66**, 56-62.
18 B. Burr and L. G. Lyddon, 2008.
19 S. Mokhatab and W. A. Poe, in *Handbook of Natural Gas Transmission and Processing (Second Edition)*, eds. S. Mokhatab and W. A. Poe, Gulf Professional Publishing, Boston, 2012, DOI: 10.1016/B978-0-12-386914-2.00007-8, pp. 253-290.
20 H. Wu, M. Shen, X. Chen, G. Yu, A. A. Abdeltawab and S. M. Yakout, *Sep. Purif. Technol.*, 2019, **224**, 281-289.
21 X. Song, Y. Zhang, C. Wu, X. Sheng and H. Zhao, *Struct. Chem.*, 2019, **30**, 2419-2428.
22 K. Huang, X.-M. Zhang, L.-S. Zhou, D.-J. Tao and J.-P. Fan, *Chem. Eng. Sci.*, 2017, **173**, 253-263.
23 W. Y. Lee, S. Y. Park, K. B. Lee and S. C. Nam, *Energy Fuels*, 2020, **34**, 1992-2000.
24 B. Wang, J. Cheng, D. Wang, X. Li, Q. Meng, Z. Zhang, J. An, X. Liu and M. Li, *ACS Omega*, 2020, **5**, 15353-15361.
25 X. Ye, S. Ma, X. Jiang, Z. Yang, W. Jiang and H. Wang, *Chin. Chem. Lett.*, 2019, **30**, 2123-2131.
26 J. Wang, L. Wang, H. Fan, H. Wang, Y. Hu and Z. Wang, *Fuel*, 2017, **209**, 329-338.
27 L. Hamon, C. Serre, T. Devic, T. Loiseau, F. Millange, G. Férey and G. D. Weireld, *J. Am. Chem. Soc.*, 2009, **131**, 8775-8777.
28 X. Liu and R. Wang, *J. Hazard. Mater.*, 2017, **326**, 157-164.
29 W. Chen, G. Zhang, D. Li, S. Ma, B. Wang and X. Jiang, *Ind. Eng. Chem. Res.*, 2020, **59**, 7447-7456.
30 D. Cortés-Arriagada, N. Villegas-Escobar and D. E. Ortega, *Appl. Surf. Sci.*, 2018, **427**, 227-236.
31 K. Chizari, A. Deneuve, O. Ersen, I. Florea, Y. Liu, D. Edouard, I. Janowska, D. Begin and C. Pham-Huu, *ChemSusChem*, 2012, **5**, 102-108.
32 S. P. Lonkar, V. Pillai, A. Abdala and V. Mittal, *RSC Adv.*, 2016, **6**, 81142-81150.
33 C. Yang, M. Florent, G. de Falco, H. Fan and T. J. Bandosz, *Chem. Eng. J.*, 2020, **394**, 124906.
34 C. A. Scholes, G. W. Stevens and S. E. Kentish, *Fuel*, 2012, **96**, 15-28.
35 W. Mazyan, A. Ahmadi, H. Ahmed and M. Hoorfar, *J. Nat. Gas Sci. Eng.*, 2016, **30**, 487-514.
36 V. P. Babu, B. E. Kraftschik and W. J. Koros, *Journal of Membrane Science*, 2018, **558**, 94-105.
37 H. Sanaeepur, A. Ebadi Amooghin, S. Bandehali, A. Moghadassi, T. Matsuura and B. Van der Bruggen, *Prog. Polym. Sci.*, 2019, **91**, 80-125.
38 Z. Liu, Y. Liu, G. Liu, W. Qiu and W. J. Koros, *Ind. Eng. Chem. Res.*, 2020, **59**, 5333-5339.
39 Z. Liu, Y. Liu, W. Qiu and W. J. Koros, *Angew. Chem.-Int. Edit.*, 2020, DOI: 10.1002/anie.202003910.
40 T. E. Rufford, S. Smart, G. C. Y. Watson, B. F. Graham, J. Boxall, J. C. Diniz da Costa and E. F. May, *Journal of Petroleum Science and Engineering*, 2012, **94-95**, 123-154.
41 A. W. Thornton, A. Ahmed, S. K. Kannam, B. D. Todd, M. Majumder and A. J. Hill, *J. Membr. Sci.*, 2015, **485**, 1-9.
42 J. G. Wijmans and R. W. Baker, *J. Membr. Sci.*, 1995, **107**, 1-21.
43 P. M. Budd, N. B. McKeown and D. Fritsch, *J. Mater. Chem.*, 2005, **15**, 1977-1986.
44 in *Materials Science of Membranes for Gas and Vapor Separation*, DOI: 10.1002/047002903X.ch5, pp. 159-189.
45 K. Ghosal and B. D. Freeman, *Polym. Adv. Technol.*, 1994, **5**, 673-697.
46 L. M. Robeson, *J. Membr. Sci.*, 1991, **62**, 165-185.
47 B. D. Freeman, *Macromolecules*, 1999, **32**, 375-380.
48 L. M. Robeson, *J. Membr. Sci.*, 2008, **320**, 390-400.
49 R. Swaidan, B. Ghanem and I. Pinnau, *ACS Macro Lett.*, 2015, **4**, 947-951.
50 B. Comesaña-Gándara, J. Chen, C. G. Bezzu, M. Carta, I. Rose, M.-C. Ferrari, E. Esposito, A. Fuoco, J. C. Jansen and N. B. McKeown, *Energy Environ. Sci.*, 2019, **12**, 2733-2740.
51 S. M. S. Niknejad, H. Savoji, M. Pourafshari Chenar and M. Soltanieh, *Int. J. Environ. Sci. Technol.*, 2017, **14**, 375-384.
52 Z. Dai, L. Ansaloni and L. Deng, *Green Energy Environ.*, 2016, **1**, 102-128.
53 M. Zhang, L. Deng, D. Xiang, B. Cao, S. S. Hosseini and P. Li, *Processes*, 2019, **7**, 51.

54 K. Vanherck, G. Koeckelberghs and I. F. J. Vankelecom, *Prog. Polym. Sci.*, 2013, **38**, 874-896.
55 M. Minelli and G. C. Sarti, *Ind. Eng. Chem. Res.*, 2020, **59**, 341-365.
56 B. Kraftschik and W. J. Koros, *Macromolecules*, 2013, **46**, 6908-6921.
57 B. Kraftschik, W. J. Koros, J. R. Johnson and O. Karvan, *J. Membr. Sci.*, 2013, **428**, 608-619.
58 J. T. Vaughn, W. J. Koros, J. R. Johnson and O. Karvan, *J. Membr. Sci.*, 2012, **401-402**, 163-174.
59 Y. Liu, Z. Liu, A. Morisato, N. Bhuwania, D. Chinn and W. J. Koros, *J. Membr. Sci.*, 2020, **601**, 117910.
60 Y. Liu, Z. Liu, G. Liu, W. Qiu, N. Bhuwania, D. Chinn and W. J. Koros, *J. Membr. Sci.*, 2020, **593**, 117430.
61 S. Yi, B. Ghanem, Y. Liu, I. Pinnau and W. J. Koros, *Sci. Adv.*, 2019, **5**, eaaw5459.
62 A. F. Ismail and W. Lorna, *Sep. Purif. Technol.*, 2002, **27**, 173-194.
63 Y. Huang and D. R. Paul, *Ind. Eng. Chem. Res.*, 2007, **46**, 2342-2347.
64 M. M. Merrick, R. Sujanani and B. D. Freeman, *Polymer*, 2020, **211**, 123176.
65 Y. Huang, X. Wang and D. R. Paul, *J. Membr. Sci.*, 2006, **277**, 219-229.
66 C. Ma and W. J. Koros, *Journal of Membrane Science*, 2018, **551**, 214-221.
67 M. Alberto, R. Bhavsar, J. M. Luque-Alled, A. Vijayaraghavan, P. M. Budd and P. Gorgojo, *J. Membr. Sci.*, 2018, **563**, 513-520.
68 C. H. Lau, P. T. Nguyen, M. R. Hill, A. W. Thornton, K. Konstas, C. M. Doherty, R. J. Mulder, L. Bourgeois, A. C. Y. Liu, D. J. Sprouster, J. P. Sullivan, T. J. Bastow, A. J. Hill, D. L. Gin and R. D. Noble, *Angew. Chem.-Int. Edit.*, 2014, **53**, 5322-5326.
69 C. H. Lau, X. Mulet, K. Konstas, C. M. Doherty, M.-A. Sani, F. Separovic, M. R. Hill and C. D. Wood, *Angew. Chem.-Int. Edit.*, 2016, **55**, 1998-2001.
70 Y. Yang, K. Goh, P. Weerachanchai and T.-H. Bae, *J. Membr. Sci.*, 2019, **574**, 235-242.
71 A. Brunetti, M. Cersosimo, G. Dong, K. T. Woo, J. Lee, J. S. Kim, Y. M. Lee, E. Drioli and G. Barbieri, *J. Membr. Sci.*, 2016, **520**, 671-678.
72 F. Almansour, M. Alberto, R. S. Bhavsar, X. Fan, P. M. Budd and P. Gorgojo, *Front. Chem. Sci. Eng.*, 2021, DOI: 10.1007/s11705-020-2001-2.
73 K. D. Dorkenoo and P. H. Pfromm, *Macromolecules*, 2000, **33**, 3747-3751.
74 C. A. Scholes, G. W. Stevens and S. E. Kentish, *AIChE J.*, 2012, **58**, 967-973.
75 Y. Liu, Z. Y. Liu, G. P. Liu, W. L. Qiu, N. Bhuwania, D. Chinn and W. J. Koros, *J. Membr. Sci.*, 2020, **593**.
76 T. Visser, G. H. Koops and M. Wessling, *Journal of Membrane Science*, 2005, **252**, 265-277.
77 E. Ricci, A. E. Gemeda, N. Du, N. Li, M. G. De Angelis, M. D. Guiver and G. C. Sarti, *J. Membr. Sci.*, 2019, **585**, 136-149.
78 E. Ricci, F. M. Benedetti, M. E. Dose, M. G. De Angelis, B. D. Freeman and D. R. Paul, *J. Membr. Sci.*, 2020, **612**, 118374.
79 J. Jansen, in *Encyclopedia of Membranes*, eds. E. Drioli and L. Giorno, Springer Berlin Heidelberg, Berlin, Heidelberg, 2016, DOI: 10.1007/978-3-642-40872-4_269-1, pp. 1-1.
80 H. T. Lu, L. Liu, S. Kanehashi, C. A. Scholes and S. E. Kentish, *J. Membr. Sci.*, 2018, **555**, 362-368.
81 C. S. K. Achoundong, N. Bhuwania, S. K. Burgess, O. Karvan, J. R. Johnson and W. J. Koros, *Macromolecules*, 2013, **46**, 5584-5594.
82 K. C. Khulbe, C. Y. Feng and J. M. A. Tan, in *Polyphenylene Oxide and Modified Polyphenylene Oxide Membranes: Gas, Vapor and Liquid Separation*, eds. G. Chowdhury, B. Kruczek and T. Matsuura, Springer US, Boston, MA, 2001, DOI: 10.1007/978-1-4615-1483-1_8, pp. 231-303.
83 S. Yi, X. Ma, I. Pinnau and W. J. Koros, *J. Mater. Chem. A*, 2015, **3**, 22794-22806.
84 X.-H. Ma and S.-Y. Yang, in *Advanced Polyimide Materials*, ed. S.-Y. Yang, Elsevier, 2018, DOI: 10.1016/B978-0-12-812640-0.00006-8, pp. 257-322.
85 N. Du, H. B. Park, M. M. Dal-Cin and M. D. Guiver, *Energy Environ. Sci.*, 2012, **5**, 7306-7322.
86 J. Vaughn and W. J. Koros, *Macromolecules*, 2012, **45**, 7036-7049.
87 J. T. Vaughn and W. J. Koros, *J. Membr. Sci.*, 2014, **465**, 107-116.
88 G. Liu, N. Li, S. J. Miller, D. Kim, S. Yi, Y. Labreche and W. J. Koros, *Angew. Chem.-Int. Edit.*, 2016, **55**, 13754-13758.
89 G. Liu, Y. Labreche, N. Li, Y. Liu, C. Zhang, S. J. Miller, V. P. Babu, N. Bhuwania and W. J. Koros, *AIChE J.*, 2019, **65**, 1269-1280.
90 G. O. Yahaya, M. S. Qahtani, A. Y. Ammar, A. A. Bahamdan, A. W. Ameen, R. H. Alhajry, M. M. Ben Sultan and F. Hamad, *Chem. Eng. J.*, 2016, **304**, 1020-1030.
91 G. O. Yahaya, I. Mokhtari, A. A. Alghannam, S. H. Choi, H. Maab and A. A. Bahamdan, *J. Membr. Sci.*, 2018, **550**, 526-535.
92 A. Hayek, G. O. Yahaya, A. Alsamah, A. A. Alghannam, S. A. Jutaily and I. Mokhtari, *Polymer*, 2019, **166**, 184-195.
93 A. A. Alghannam, G. O. Yahaya, A. Hayek, I. Mokhtari, Q. Saleem, D. A. Sewdan and A. A. Bahamdan, *Journal of Membrane Science*, 2018, **553**, 32-42.
94 A. Hayek, G. O. Yahaya, A. Alsamah and S. K. Panda, *J. Appl. Polym. Sci.*, 2020, **137**.
95 G. O. Yahaya, S. H. Choi, M. M. Ben Sultan and A. Hayek, *Glob. Chall.*, 2020, **4**.
96 A. Hayek, A. Alsamah, G. O. Yahaya, E. A. Qasem and R. H. Alhajry, *J. Mater. Chem. A*, 2020, **8**, 23354-23367.
97 A. Hayek, A. Alsamah, E. A. Qasem, N. Alaslai, R. H. Alhajry and G. O. Yahaya, *Sep. Purif. Technol.*, 2019, **227**.
98 A. Hayek, A. Alsamah, N. Alaslai, H. Maab, E. A. Qasem, R. H. Alhajry and N. M. Alyami, *ACS Appl. Polym. Mater.*, 2020, **2**, 2199-2210.
99 G. Dong and Y. M. Lee, *J. Mater. Chem. A*, 2017, **5**, 13294-13319.
100 N. B. McKeown and P. M. Budd, *Macromolecules*, 2010, **43**, 5163-5176.
101 N. B. McKeown, *Polymer*, 2020, **202**, 122736.
102 P. M. Budd, B. S. Ghanem, S. Makhseed, N. B. McKeown, K. J. Msayib and C. E. Tattershall, *Chem. Commun.*, 2004, DOI: 10.1039/B311764B, 230-231.

103 P. M. Budd, N. B. McKeown, B. S. Ghanem, K. J. Msayib, D. Fritsch, L. Starannikova, N. Belov, O. Sanfirova, Y. Yampolskii and V. Shantarovich, *J. Membr. Sci.*, 2008, **325**, 851-860.
104 P. M. Budd, K. J. Msayib, C. E. Tattershall, B. S. Ghanem, K. J. Reynolds, N. B. McKeown and D. Fritsch, *J. Membr. Sci.*, 2005, **251**, 263-269.
105 M. D. Guiver and Y. M. Lee, *Science*, 2013, **339**, 284.
106 E. Ghasemnejad-Afshar, S. Amjad-Iranagh, M. Zarif and H. Modarress, *Polym. Test*, 2020, **83**, 106339.
107 X. Ma, R. Swaidan, Y. Belmabkhout, Y. Zhu, E. Litwiller, M. Jouiad, I. Pinnau and Y. Han, *Macromolecules*, 2012, **45**, 3841-3849.
108 M. Sadeghi, M. M. Talakesh, A. Arabi Shamsabadi and M. Soroush, *ChemistrySelect*, 2018, **3**, 3302-3308.
109 R. R. Tiwari, J. Jin, B. D. Freeman and D. R. Paul, *J. Membr. Sci.*, 2017, **537**, 362-371.
110 J. A. Lawrence, D. J. Harrigan, C. R. Maroon, S. A. Sharber, B. K. Long and B. J. Sundell, *Journal of Membrane Science*, 2020, **616**.
111 B. J. Sundell, J. A. Lawrence Iii, D. J. Harrigan, J. T. Vaughn, T. S. Pilyugina and D. R. Smith, *RSC Adv.*, 2016, **6**, 51619-51628.
112 C. R. Maroon, J. Townsend, K. R. Gmernicki, D. J. Harrigan, B. J. Sundell, J. A. Lawrence, S. M. Mahurin, K. D. Vogiatzis and B. K. Long, *Macromolecules*, 2019, **52**, 1589-1600.
113 C. R. Maroon, J. Townsend, M. A. Higgins, D. J. Harrigan, B. J. Sundell, J. A. Lawrence, J. T. O'Brien, D. O'Neal, K. D. Vogiatzis and B. K. Long, *J. Membr. Sci.*, 2020, **595**, 117532.
114 T. C. Merkel, R. P. Gupta, B. S. Turk and B. D. Freeman, *J. Membr. Sci.*, 2001, **191**, 85-94.
115 K. Golzar, H. Modarress and S. Amjad-Iranagh, *J. Membr. Sci.*, 2017, **539**, 238-256.
116 T. Li, Y. Pan, K.-V. Peinemann and Z. Lai, *J. Membr. Sci.*, 2013, **425-426**, 235-242.
117 S. Claes, P. Vandezande, S. Mullens, R. Leysen, K. De Sitter, A. Andersson, F. H. J. Maurer, H. Van den Rul, R. Peeters and M. K. Van Bael, *J. Membr. Sci.*, 2010, **351**, 160-167.
118 S. He, X. Jiang, S. Li, F. Ran, J. Long and L. Shao, *AIChE J.*, 2020, **66**, e16543.
119 D. F. Sanders, Z. P. Smith, R. Guo, L. M. Robeson, J. E. McGrath, D. R. Paul and B. D. Freeman, *Polymer*, 2013, **54**, 4729-4761.
120 K. Ghasemzadeh, S. M. Sadati Tilebon and A. Basile, in *Current Trends and Future Developments on (Bio-) Membranes*, eds. A. Basile and E. P. Favvas, Elsevier, 2018, DOI: 10.1016/B978-0-12-813645-4.00018-0, pp. 511-549.
121 G. Chatterjee, A. A. Houde and S. A. Stern, *J. Membr. Sci.*, 1997, **135**, 99-106.
122 T. Mohammadi, M. T. Moghadam, M. Saeidi and M. Mahdyarfar, *Ind. Eng. Chem. Res.*, 2008, **47**, 7361-7367.
123 W. J. Koros and C. Zhang, *Nat. Mater.*, 2017, **16**, 289-297.
124 D. J. Harrigan, J. A. Lawrence, H. W. Reid, J. B. Rivers, J. T. O'Brien, S. A. Sharber and B. J. Sundell, *J. Membr. Sci.*, 2020, **602**, 117947.
125 S. Saedi, S. S. Madaeni and A. A. Shamsabadi, *Can. J. Chem. Eng,*, 2014, **92**, 892-904.
126 Y. Mansourpanah, S. S. Madaeni and A. Rahimpour, *J. Membr. Sci.*, 2009, **343**, 219-228.
127 A. Rahimpour, S. S. Madaeni and Y. Mansourpanah, *J. Membr. Sci.*, 2007, **296**, 110-121.
128 A. Rahimpour and S. S. Madaeni, *J. Membr. Sci.*, 2007, **305**, 299-312.
129 B. Zhu, X. Jiang, S. He, X. Yang, J. Long, Y. Zhang and L. Shao, *J. Mater. Chem. A*, 2020, **8**, 24233-24252.
130 X. Jiang, S. Li and L. Shao, *Energy Environ. Sci.*, 2017, **10**, 1339-1344.
131 X. Jiang, S. He, S. Li, Y. Bai and L. Shao, *J. Mater. Chem. A*, 2019, **7**, 16704-16711.
132 H. Zhao, X. Ding, P. Yang, L. Li, X. Li and Y. Zhang, *J. Membr. Sci.*, 2015, **489**, 258-263.
133 Y. Liu, Z. Liu, B. E. Kraftschik, V. P. Babu, N. Bhuwania, D. Chinn and W. J. Koros, *J. Membr. Sci.*, 2021, **632**, 119361.
134 M. Bhattacharya and M. K. Mandal, *J. Clean Prod.*, 2017, **156**, 174-183.
135 G. P. Liu, V. Chernikova, Y. Liu, K. Zhang, Y. Belmabkhout, O. Shekhah, C. Zhang, S. L. Yi, M. Eddaoudi and W. J. Koros, *Nat. Mater.*, 2018, **17**, 283-+.
136 Y. Li, G. He, S. Wang, S. Yu, F. Pan, H. Wu and Z. Jiang, *J. Mater. Chem. A*, 2013, **1**, 10058-10077.
137 J. Ahmad and M.-B. Hägg, *J. Membr. Sci.*, 2013, **427**, 73-84.
138 N. Norahim, K. Faungnawakij, A. T. Quitain and C. Klaysom, *J. Chem. Technol. Biotechnol.*, 2019, **94**, 2783-2791.
139 H. M. Rizwan Nasir, Zakaria Man, Maizatul Shima Shaharun, Mohamad Zailani Abu Bakar, *Chem. Eng. Trans.*, 2015, **45**, 1417-1422.
140 M. Z. Ahmad, T. A. Peters, N. M. Konnertz, T. Visser, C. Téllez, J. Coronas, V. Fila, W. M. de Vos and N. E. Benes, *Sep. Purif. Technol.*, 2020, **230**, 115858.
141 M. Nour, K. Berean, A. Chrimes, A. S. Zoolfakar, K. Latham, C. McSweeney, M. R. Field, S. Sriram, K. Kalantar-zadeh and J. Z. Ou, *Journal of Membrane Science*, 2014, **470**, 346-355.
142 Z. Qiao, Q. Xu and J. Jiang, *J. Mater. Chem. A*, 2018, **6**, 18898-18905.
143 S. M. Wang, D. Wu, H. L. Huang, Q. Y. Yang, M. M. Tong, D. H. Liu and C. L. Zhong, *Chin. J. Chem. Eng.*, 2015, **23**, 1291-1299.
144 N. Jadhav, S. N. Kumar, P. S. Tanvidkar and B. V. R. Kuncharam, *Mater. Today*, 2020, **28**, 734-738.
145 S. Øien, D. Wragg, H. Reinsch, S. Svelle, S. Bordiga, C. Lamberti and K. P. Lillerud, *Cryst. Growth Des.*, 2014, **14**, 5370-5372.
146 Q. Yang, A. D. Wiersum, H. Jobic, V. Guillerm, C. Serre, P. L. Llewellyn and G. Maurin, *The Journal of Physical Chemistry C*, 2011, **115**, 13768-13774.
147 M. Zamidi Ahmad, M. Navarro, M. Lhotka, B. Zornoza, C. Téllez, V. Fila and J. Coronas, *Sep. Purif. Technol.*, 2018, **192**, 465-474.
148 T. C. Merkel, B. D. Freeman, R. J. Spontak, Z. He, I. Pinnau, P. Meakin and A. J. Hill, *Science*, 2002, **296**, 519.
149 G. Liu, A. Cadiau, Y. Liu, K. Adil, V. Chernikova, I.-D. Carja, Y. Belmabkhout, M. Karunakaran, O. Shekhah, C. Zhang, A. K. Itta, S. Yi, M. Eddaoudi and W. J. Koros, *Angew. Chem.-Int. Edit.*, 2018, **57**, 14811-14816.
150 L. Crowhurst, P. R. Mawdsley, J. M. Perez-Arlandis, P. A. Salter and T. Welton, *Phys. Chem. Chem. Phys.*, 2003, **5**, 2790-2794.
151 D. R. MacFarlane and K. R. Seddon, *Aust. J. Chem.*, 2007, **60**, 3-5.

152 A. H. Jalili, M. Rahmati-Rostami, C. Ghotbi, M. Hosseini-Jenab and A. N. Ahmadi, *Journal of Chemical & Engineering Data*, 2009, **54**, 1844-1849.
153 C. S. Pomelli, C. Chiappe, A. Vidis, G. Laurenczy and P. J. Dyson, *J. Phys. Chem. B*, 2007, **111**, 13014-13019.
154 X.-M. Zhang, K. Huang, S. Xia, Y.-L. Chen, Y.-T. Wu and X.-B. Hu, *Chem. Eng. J.*, 2015, **274**, 30-38.
155 P. K. Parhi, *J. Chem.*, 2013, **2013**, 618236.
156 S. Uk Hong, D. Park, Y. Ko and I. Baek, *Chem. Commun.*, 2009, DOI: 10.1039/B913746G, 7227-7229.
157 B. A. Voss, J. E. Bara, D. L. Gin and R. D. Noble, *Chem. Mat.*, 2009, **21**, 3027-3029.
158 D. Camper, J. Bara, C. Koval and R. Noble, *Ind. Eng. Chem. Res.*, 2006, **45**, 6279-6283.
159 Y.-I. Park, B.-S. Kim, Y.-H. Byun, S.-H. Lee, E.-W. Lee and J.-M. Lee, *Desalination*, 2009, **236**, 342-348.
160 X. Zhang, Z. Tu, H. Li, K. Huang, X. Hu, Y. Wu and D. R. MacFarlane, *J. Membr. Sci.*, 2017, **543**, 282-287.
161 F. J. Hernández-Fernández, A. P. de los Ríos, F. Tomás-Alonso, J. M. Palacios and G. Víllora, *J. Membr. Sci.*, 2009, **341**, 172-177.
162 A. I. Akhmetshina, N. R. Yanbikov, A. A. Atlaskin, M. M. Trubyanov, A. Mechergui, K. V. Otvagina, E. N. Razov, A. E. Mochalova and I. V. Vorotyntsev, *Membranes*, 2019, **9**.
163 A. H. Jalili, A. Mehdizadeh, M. Shokouhi, A. N. Ahmadi, M. Hosseini-Jenab and F. Fateminassab, *J. Chem. Thermodyn.*, 2010, **42**, 1298-1303.
164 S. N. V. K. Aki, B. R. Mellein, E. M. Saurer and J. F. Brennecke, *J. Phys. Chem. B*, 2004, **108**, 20355-20365.
165 K. Huang, D.-N. Cai, Y.-L. Chen, Y.-T. Wu, X.-B. Hu and Z.-B. Zhang, *AIChE J.*, 2013, **59**, 2227-2235.
166 P. Scovazzo, A. E. Visser, J. H. Davis, R. D. Rogers, C. A. Koval, D. L. DuBois and R. D. Noble, in *Ionic Liquids*, American Chemical Society, 2002, vol. 818, ch. 6, pp. 69-87.
167 J. L. Anthony, E. J. Maginn and J. F. Brennecke, *J. Phys. Chem. B*, 2002, **106**, 7315-7320.
168 J. L. Anthony, J. L. Anderson, E. J. Maginn and J. F. Brennecke, *J. Phys. Chem. B*, 2005, **109**, 6366-6374.
169 J. Jacquemin, M. F. Costa Gomes, P. Husson and V. Majer, *J. Chem. Thermodyn.*, 2006, **38**, 490-502.
170 P. Husson-Borg, V. Majer and M. F. Costa Gomes, *J. Chem. Eng. Data*, 2003, **48**, 480-485.
171 Y. Hou and R. E. Baltus, *Ind. Eng. Chem. Res.*, 2007, **46**, 8166-8175.
172 A. M. O'Mahony, E. J. F. Dickinson, L. Aldous, C. Hardacre and R. G. Compton, *The Journal of Physical Chemistry C*, 2009, **113**, 10997-11002.
173 M. B. Shiflett, D. J. Kasprzak, C. P. Junk and A. Yokozeki, *J. Chem. Thermodyn.*, 2008, **40**, 25-31.
174 D. D. Iarikov, P. Hacarlioglu and S. T. Oyama, *Chem. Eng. J.*, 2011, **166**, 401-406.
175 A. Alkhouzaam, M. Khraisheh, M. Atilhan, S. A. Al-Muhtaseb, L. Qi and D. Rooney, *J. Nat. Gas Sci. Eng.*, 2016, **36**, 472-485.
176 M. Wang, D. Yang, Z. Wang, J. Wang and S. Wang, *Front. Chem. Eng. China*, 2010, **4**, 127-132.
177 X. Jiang, S. He, G. Han, J. Long, S. Li, C. H. Lau, S. Zhang and L. Shao, *ACS Appl. Mater. Interfaces*, 2021, **13**, 11296-11305.
178 S. Hwang, W. S. Chi, S. J. Lee, S. H. Im, J. H. Kim and J. Kim, *J. Membr. Sci.*, 2015, **480**, 11-19.
179 M. Mozafari, R. Abedini and A. Rahimpour, *J. Mater. Chem. A*, 2018, **6**, 12380-12392.
180 R. Khalilpour, K. Mumford, H. Zhai, A. Abbas, G. Stevens and E. S. Rubin, *J. Clean Prod.*, 2015, **103**, 286-300.
181 I. Iliuta and M. C. Iliuta, *Ind. Eng. Chem. Res.*, 2015, **54**, 12455-12465.
182 Y. Zhang and R. Wang, *Curr. Opin. Chem. Eng.*, 2013, **2**, 255-262.
183 O. Falk-Pedersen, M. S. Gronvold, P. Nokleby, F. Bjerve and H. F. Svendsen, *Int. J. Green Energy*, 2005, **2**, 157-165.
184 S. A. M. Marzouk, M. H. Al-Marzouqi, M. Teramoto, N. Abdullatif and Z. M. Ismail, *Sep. Purif. Technol.*, 2012, **86**, 88-97.
185 S. A. M. Marzouk, M. H. Al-Marzouqi, N. Abdullatif and Z. M. Ismail, *J. Membr. Sci.*, 2010, **360**, 436-441.
186 R. Faiz, K. Li and M. Al-Marzouqi, *Chem. Eng. Process.*, 2014, **83**, 33-42.
187 P. Tantikhajorngosol, N. Laosiripojana, R. Jiraratananon and S. Assabumrungrat, *Int. J. Heat Mass Transf.*, 2019, **128**, 1136-1148.
188 M. H. Al-Marzouqi, S. A. M. Marzouk and N. Abdullatif, *Journal of Natural Gas Science and Engineering*, 2017, **37**, 192-198.
189 W. Rongwong, S. Boributh, S. Assabumrungrat, N. Laosiripojana and R. Jiraratananon, *J. Membr. Sci.*, 2012, **392-393**, 38-47.
190 Z. Pan, N. Zhang, W. Zhang and Z. Zhang, *J. Clean Prod.*, 2020, **273**, 123107.
191 S. M. Mirfendereski, Z. Niazi and T. Mohammadi, *Chem. Eng. Technol.*, 2019, **42**, 196-208.
192 K. Simons, K. Nijmeijer and M. Wessling, *J. Membr. Sci.*, 2009, **340**, 214-220.
193 Y. Li, L. a. Wang, X. Hu, P. Jin and X. Song, *Sep. Purif. Technol.*, 2018, **194**, 222-230.
194 R. Faiz and M. Al-Marzouqi, *J. Membr. Sci.*, 2010, **365**, 232-241.
195 A. Zolfaghari, S. A. Mousavi, R. B. Bozarjomehri and F. Bakhtiari, *J. Membr. Sci.*, 2018, **555**, 463-472.
196 S. Kim, C. A. Scholes, D. E. Heath and S. E. Kentish, *Chem. Eng. J.*, 2021, **411**, 128468.
197 H. Abdolahi-Mansoorkhani and S. Seddighi, *Energy*, 2019, **168**, 847-857.
198 Y. Lv, X. Yu, J. Jia, S.-T. Tu, J. Yan and E. Dahlquist, *Appl. Energy*, 2012, **90**, 167-174.
199 E. Tilahun, A. Bayrakdar, E. Sahinkaya and B. Çalli, *Waste Manage.*, 2017, **61**, 250-257.
200 M. Hedayat, M. Soltanieh and S. A. Mousavi, *J. Membr. Sci.*, 2011, **377**, 191-197.
201 R. Sakwattanapong, A. Aroonwilas and A. Veawab, *Ind. Eng. Chem. Res.*, 2005, **44**, 4465-4473.
202 M. Wang, A. S. Joel, C. Ramshaw, D. Eimer and N. M. Musa, *Appl. Energy*, 2015, **158**, 275-291.
203 K. A. Mumford, Y. Wu, K. H. Smith and G. W. Stevens, *Front. Chem. Sci. Eng.*, 2015, **9**, 125-141.
204 S. Yan, Q. He, S. Zhao, Y. Wang and P. Ai, *Chem. Eng. Process.*, 2014, **85**, 125-135.

205 A. Taghvaie Nakhjiri, A. Heydarinasab, O. Bakhtiari and T. Mohammadi, *J. Environ, Chem. Eng.*, 2020, **8**, 104130.
206 A. Bahlake, F. Farivar and B. Dabir, *Heat Mass Transf.*, 2016, **52**, 1295-1304.
207 S. Mohebi, S. M. Mousavi and S. Kiani, *Journal of Natural Gas Science and Engineering*, 2009, **1**, 195-204.
208 A. Esquiroz-Molina, S. Georgaki, R. Stuetz, B. Jefferson and E. J. McAdam, *Journal of Membrane Science*, 2013, **427**, 276-282.
209 R. Faiz and M. Al-Marzouqi, *Sep. Purif. Technol.*, 2011, **76**, 351-361.
210 R. Faiz and M. Al-Marzouqi, *J. Membr. Sci.*, 2010, **350**, 200-210.
211 P. Tantikhajorngosol, N. Laosiripojana, R. Jiraratananon and S. Assabumrungrat, *J. Membr. Sci.*, 2018, **549**, 283-294.
212 R. Faiz and M. Al-Marzouqi, *J. Membr. Sci.*, 2009, **342**, 269-278.
213 L. Ansaloni, A. Hartono, M. Awais, H. K. Knuutila and L. Deng, *Chem. Eng. J.*, 2019, **359**, 1581-1591.
214 L. Ansaloni, R. Rennemo, H. K. Knuutila and L. Deng, *J. Membr. Sci.*, 2017, **537**, 272-282.
215 M. Ahmadi, A. Lindbråthen, M. Hillestad and L. Deng, *Chem. Eng. J.*, 2021, **404**, 126535.

PostPrint: Yulei Ma, et al., Journal of Materials Chemistry A, 2021, **9**, 20211-20240
https://doi.org/10.1039/D1TA04693D